Measuring suspended sediments in periglacial reservoirs using water samples, LISST and ADCP

Ehrbar, D., Doering, M., Schmocker, L., Vetsch, D.F., Boes, R.M.

ABSTRACT Climate change will impact the water and sediment conveyance into periglacial reservoirs. It is therefore important to understand and forecast future reservoir sedimentation processes with regard to climate change. In the present project, particle size distribution (PSD) and suspended sediment concentrations (SSC) were measured in three reservoirs in the Swiss Alps whose catchment areas are covered by glaciers by at least 40%. The threefold combination of water sample analysis, laser in-situ scattering and transmissometry (LISST) and acoustic Doppler current profiler (ADCP) was applied and the results compared to each other. The combination of the three measuring techniques was proven suitable for assessing PSD and SSC in periglacial reservoirs. Water sample analysis and LISST records showed that most of the suspended sediments in the reservoir are in the range of clay and silt. SSC was relatively low in the order of 100 mg/l. An increase of both PSD (e.g. median diameter d_{50}) and SSC with increasing reservoir depth could be observed in deep reservoirs. Flow velocities and Signal-to-Noise ratios (SNR) were measured with ADCP. SNR values allowed to study the mixing of inflowing river water and the evolution and decay of turbidity currents. There is evidence of dominant homopycnal flows, i.e. stratified flow was restricted to the regions close to the inflow. Flocculation, influence of mica, and organic content could be neglected. This paper presents detailed information about PSD and SSC gained with water sample analysis and LISST measurements. Furthermore, flow field measurements and tracking of mixing by means of ADCP will be illustrated. Finally, application experiences and limitations will be discussed.

Keywords: periglacial reservoir, laser in-situ scattering transmissometry (LISST), acoustic Doppler current profiler (ADCP), particle size distribution (PSD), suspended sediment concentration (SSC), Signal-to-Noise ratio (SNR)

1. Introduction

Since 1880, temperature has risen by 0.85°C worldwide (IPCC 2013). In Switzerland, a more pronounced temperature increase of 1.8°C has been observed since 1864 (SCNAT 2016). Due to this atmospheric warming, glacier area was reduced from 1300 km^2 in 1973 to 940 km^2 in 2010 (SCNAT 2016). For the two non-intervention emission scenarios A2 and A1B (IPCC 2013), increases of seasonal mean temperature of 3.2–4.8°C (A2 scenario) and 2.7–4.1°C (A1B scenario) are expected until the end of the century compared to the past 30 years. For the climate stabilisation scenario RCP3PD, a warming of 1.2–1.8°C is expected (CH2011). Swiss glaciers will then cover only ca. 300 km^2 (SGHL & CHy 2011).

Impacts of climate change on runoff in Swiss catchments has been examined at different scales. Addor et al. (2014) found a general pattern valid for six mesoscale catchments: (i) lower summer (June, July, August) flows ("damping"), (ii) earlier timing of spring-summer peak discharge ("shifting"), and (iii) larger winter (December, January, February) flows ("flattening"). Farinotti et al. (2012) investigated nine high-alpine catchments and claim that precipitation will remain almost unaltered in inner-Alpine regions, but that there will be a transition from glacial and glacio-nival regimes to nival regimes. This transition mainly depends on the degree of glaciation, the total ice volume present today and the distribution of ice with altitude. Climate change impact at the single catchment or glacier scale have been studied e.g. by Gabbi et al. (2012), Huss et al. (2008a,b; 2014), Jouvet et al. (2011) or Uhlmann et al. (2013). Huss et al. (2014) showed for Findelengletscher that the overall uncertainties in annual runoff due to (a) the spread in regional climate models and (b) glacio-hydrological models are in the range of -57% to +25%. August runoff has overall uncertainties of -94% to -5%.

Different processes and timescales govern periglacial sediment yield (Guillon 2016). Beyer-Portner (1998) found a correlation between annual sediment yield and mean precipitation in summer, the catchment share in soils prone to erosion, the catchment share without vegetation cover and the relative annual length change of the glaciers in the catchment. Gurnell et al. (1996) examined 72 glacier basins worldwide and found that annual suspended sediment yield correlates with annual water discharge volume. The time series of suspended sediment yield ranged from 1 to 82 years. Felix (2017), however, did not find such a correlation for the highly glaciated

Fiescher catchment in the Swiss Alps for the years 2012-2014 including a 20-year flood. Subglacial drainage plays an essential role in periglacial environments. Swift et al. (2005) found that in winter suspended sediment concentrations (SSC) in meltwater streams are proportional to the water discharge to the power of 1.3, whereas they are proportional to the power of 2.2 in summer. They identified the glacial drainage system as the main cause for this feature: in winter, only slow and inefficient distributed systems (e.g. sheets, films, cavities) are present; whereas in summer, fast and efficient channelized systems (e.g. Nye or Röthlisberger channels) are established. In addition, subglacial storage has to be taken into account, as Riihimaki et al. (2005) showed.

Furthermore, glacier retreat may lead to large, bare forefields that are easily erodible due to the lack of vegetation. The eroded sediments are conveyed into the reservoir where they deposite to a large extent (Geilhausen et al. 2013). 70 to 100% of these sediments are suspended load (Jenzer Althaus 2011), which can be distributed in the whole lake. Suspended sediment yield is considered supply-controlled, i.e. hydraulic conditions are of minor importance (Stott & Mount 2007). Therefore, sediment conveyance into these reservoirs may likely increase significantly as bare glacier forefields grow. Micheletti & Lane (2016) compared sediment export and sediment transport capacities in two Alpine watersheds and concluded that transport is mainly determined by connectivity and not by availability, i.e. large sediment production does not necessarily lead to large sediment export. They claim that the latter is linked with significant events such as heavy rainfalls or debris flows. In summary, it can be assumed that sediment yield from periglacial catchments will change due to climate change.

Reservoir sedimentation is a major issue for reservoirs close to the glacial environment. Several reservoirs in the Swiss Alps exhibit large sedimentation rates. Gebidem, the reservoir downstream of Grosser Aletschgletscher, has an infill time (time until the reservoir is completely filled with sediment) of 22 to 24 years (Meile et al. 2014). Worldwide, net storage is currently decreasing because the sedimentation rate is increasing faster than new storage is installed (Auel & Boes 2012). Reservoir sedimentation leads to annual worldwide replacement investments of 13 to 19 trillion (1E12) US-$ (Schleiss et al. 2010). Reservoir lifetime and sustainability are often governed by sedimentation (Wisser et al. 2013).

Reservoir sedimentation is determined based on the sediment fluxes in the lake. Governing parameters include particle size distribution (PSD), suspended sediment concentration (SSC) or flow velocities. Recent innovations, such as laser in-situ scattering transmissometry (LISST) or acoustic Doppler current profiler (ADCP), provide new measuring techniques for the acquisition of these sediment data. Both techniques can be applied either in moving mode (e.g. from a boat) or in stationary mode (e.g. fixed at an intake). So far, only few applications of LISST and ADCP in glacier-fed mountain lakes are reported: Kostaschuk et al. (2005) applied ADCP in moving mode, Hodder & Gilbert (2007) and Hodder (2009) applied LISST in moving mode, and Menczel & Kostaschuk (2013) applied both ADCP in moving mode and LISST in stationary mode. One reason for the few applications is the fact that these techniques require an accurate calibration and validation with e.g. water samples. In the scope of this project, PSD and SSC in three Swiss reservoirs were studied. The combination of water samples, LISST and ADCP was applied systematically to gain profound insights into PSD and SSC in reservoirs in the periglacial environment, where field data is still scarce. In different environments, this threefold combination has been applied in several studies: Haun & Lizano (2015) measured sediment fluxes in a reservoir in Costa Rica and tracked density currents (Haun & Lizano 2016); Lee et al. (2016) studied a river plume in Taiwan; Duclos et al. (2013) examined dredging plumes in the Bay of Seine; Fettweis et al. (2006), Bartholomä et al. (2009) and Santos et al. (2014) investigated sediment transport processes in the Belgian coastal zone, the German Wadden Sea and in an inner shelf of Portugal, respectively. Tidal currents and their impacts on sedimentation and resuspension were studied by Yuan et al. (2008) or Unverricht et al. (2014) in Jiaozhou Bay and Mekong Delta, respectively. Ha et al. (2015) measured suspended sediments under ice in the Arctic Ocean. These studies demonstrate the wide application range of LISST and ADCP.

In this paper, LISST and ADCP measurements carried out in three periglacial reservoirs in Switzerland are presented and discussed. Data were acquired during measuring campaigns in summer and autumn 2015 and 2016 under different inflow conditions. The variability and commonalities are presented and the LISST and ADCP data are compared with water samples. Limitations of the measuring techniques are shown and application experiences are given.

2. Methods

2.1 Measuring campaign

Three periglacial reservoirs (Lac de Mauvoisin, Griessee and Gebidem) with different characteristics were selected for field measurements. All three reservoirs have a catchment glaciation share of at least 40%. The glaciers will be subject to both strong mass balance and length changes in the next decades, which will have impacts on the reservoirs. Both water samples as well as LISST profiles were collected in all reservoirs. ADCP measurements were carried out in Griessee and Gebidem. The ADCP measurements from Gebidem had to be discarded, because the narrow gorge did not allow a proper GPS positioning of the device. ADCP was always continuously recording throughout the whole measuring campaign at Griessee. Average boat speed during ADCP measurements was 4.1 km/h (18 August 2015) and 4.4 km/h (8 August 2016), respectively. Each transect was measured only once. The boat was stopped at certain positions to record LISST profiles. LISST was lowered manually with a speed of approximately 0.1 m/s. Afterwards, water samples were taken at the same location at different depths.

2.1.1 Lac de Mauvoisin

Lac de Mauvoisin (WGS84 45.99803, 7.34883) is a large annual storage reservoir situated in the Pennine Alps. First impounding took place in 1956. Full supply level is at 1975 m a.s.l., drawdown level is at 1825 m a.s.l. Maximum depth is ca. 180 m. The lake surface area is 2.26 km^2, the total reservoir volume is 204 hm^3. The catchment has a size of 150 km^2, of which 42% are covered by glaciers (Gabbi et al. 2012). Schleiss et al. (1996) estimated an annual sedimentation volume of 330'000 m^3. The corresponding infill time equals 618 years. The field measurements presented in this paper were realized on 11 August 2015. That day, average inflow was 29.7 m^3/s, the lake level was at 1966.9 m a.s.l., and water temperature was 6.1–6.4°C.

2.1.2 Griessee

Griessee (WGS84 46.46132, 8.37067) is one of the highest reservoir locations in Switzerland. First impounding took place in 1967. The catchment has a size of 10 km^2, of which 47% are covered by glaciers (Farinotti et al. 2012). Full supply level is at 2386.5 m a.s.l., drawdown level is at 2350 m a.s.l. Maximum depth is ca. 66 m. The lake surface area is 0.6 km^2, the total reservoir volume is 18 hm^3. Between 1976 and 2011, 618'240 m^3 of sediment were deposited in Griessee (Beck & Baron 2011), while 169'061 m^3 between 2011 and 2015 (Beck & Baron 2015). Corresponding infill times are 1019 years and 426 years, respectively. Until 1986, the tongue of Gries glacier reached into the reservoir. Since then, it has been retreating considerably, exposing a growing proglacial area between the glacier tongue and the reservoir (Delaney et al. 2016). This evolution of the proglacial area due to atmospheric warming may be the reason for the significantly lower infill times observed in recent years. Three measuring campaigns on 18 August 2015, 1 October 2015 and 8 August 2016 will be discussed in this paper. The measurements in August 2015 and 2016 can be interpreted as "summer state", while the measurements of 1 October 2015 correspond to a "winter state". On 18 August 2015, the inflow was moderate with a peak of 1.5 m^3/s as it was a cold and rainy day. On 8 August 2016, the inflow was high with a peak of 5.6 m^3/s early in the afternoon because of high temperatures and clear sky. The lake level was at 2373.3 m a.s.l. and 2379.0 m a.s.l. and water temperatures were 6.3–6.4°C and 6.0–6.4°C, respectively. On 1 October 2015, there was negligible inflow as it was snowing. The lake level was at 2383.2 m a.s.l, and water temperature was 5.1–5.3°C.

2.1.3 Gebidem

Gebidem (WGS84 46.37118, 8.00241) has a strong sedimentation rate and the infill time is estimated in the range of 22 to 24 years (Meile et al. 2014). It is located in the Massa gorge downstream of Grosser Aletschgletscher, the largest Alpine glacier. First impounding took place in 1964. Full supply level is at 1436.5 m a.s.l., drawdown level is at 1400 m a.s.l. Maximum depth is ca. 104 m. The lake surface area is 0.21 km^2, the total reservoir volume is 9.2 hm^3. The catchment has a size of 198 km^2, of which 64% are covered by glaciers (Meile et al. 2014). According to Meile et al. (2014), the annual sedimentation volume since 2001 is 387'000 m^3 to 423'000 m^3. The corresponding infill time is 22 to 24 years. The measurements of 6 October 2015 will be discussed in this paper. That day, inflow was ca. 11 m^3/s, the lake level was at 1431.51 m a.s.l, and water temperature was 1.4–2.0°C.

2.2 Measuring techniques

2.2.1 Water sample analysis

Water samples were used to determine PSD and SSC at different locations and depths. Samples were taken in the inflowing river and in the reservoir with a 2 liter Niskin bottle sampler. The sampling locations correspond to the position of LISST profiles and ADCP transects.

Taking water samples is done by dropping a weight ("messenger") down the cable of the Niskin bottle. The impact of the weight closes the caps and seals the water in the bottle. At large depths of more than 20 m, the impact is not strong enough to release the caps. Therefore, sampling depths are limited to approximately 20 m. Due to limited boat load and operation space, no larger device could be applied.

PSD was analysed using a Horiba Partica LA-950 laser diffraction particle size distribution analyser. SSC was measured based on drying and weighing, using a Mettler Toledo XPE205 high-precision balance.

PSD was measured using two procedures, depending on the SSC. High SSC (SSC > 1 g/l) made direct measurement of PSD from the water sample possible. Low SSC (SSC < 1 g/l) required that the suspension had to be thickened first by evaporating the water sample at 65°C in an oven. Long storage times in the climate chamber or the evaporating lead in a few cases to the formation of flocs. These flocs were destroyed with ultrasounding. No anti-coagulation fluid had to be applied. The majority of water samples did not show any sign of flocculation, i.e. the results were not affected by ultrasounding. Water samples being analysed shortly after acquisition were not affected by flocculation. The laser diffraction analyser has a dynamic range from 0.01 to 3000 µm. All samples showed PSD completely in this range.

SSC was measured with a basic weighing procedure. First, a cling film was weighed with the balance. Second, this cling film was put into a porcelain dish, which was then filled with 1 liter of sample water. Third, this probe was dried in the oven at 65°C for at least three days. Fourth, cling film and remaining sediments were weighed again and SSC was calculated. Usually, SSC weight was less than 10% of the weight of the cling film. Laboratory analysis of SSC depends on the accuracy of the weighing, as most of the weight is represented by the cling film and not the remaining sediment.

2.2.2 LISST measurements

Laser in-situ scattering and transmissometry (LISST) is a product name introduced by Sequoia Scientific. It denotes a submersible particle size analyser, allowing simultaneous measurement of both PSD and SSC. In this study, a LISST-100X Type C was applied. It has a maximum operating depth of 300 m. The randomly shaped particle inversion method was used in the post-processing. Operating ranges are limited to particle sizes between 1.9 and 381 µm and concentrations between 1 and 750 mg/l, approximately. A 90% path reduction module (PRM) allowed measuring higher concentrations. It was applied in 2015 and removed in 2016, i.e. all measurements except the data from 8 August 2016 were recorded with the PRM. The installation of a PRM needs careful attention and could not be carried out on the boat. Therefore, a direct comparison of field measurements at the same location and day with and without PRM was impossible. Additional measuring parameters apart from PSD and SSC are, amongst others, beam attenuation, depth and temperature. The device was slowly lowered manually to the bottom of the reservoir. Operating mode was set at fixed sample rates of 1 s. Both measurements while lowering and lifting the instrument were recorded.

General operating principles and applications of LISST are described e.g. in Agrawal & Pottsmith (1994, 2000), Agrawal et al. (2008), and Andrews et al. (2011b). Application ranges and accuracy of LISST are given e.g. in Felix et al. (2013). According to Haun et al. (2015), LISST devices should be applied in an optical transmission range between 0.3 and 0.98. Measurements of the top 1 m were neglected to avoid erroneous measurements due to ambient light (Andrews et al. 2011a). Sediment density was assumed to 2650 kg/m^3.

Flocculation effects are not taken into account because the large majority of water samples did not have flocs (section 2.2.1). It is almost impossible to determine flocs in the field because their size is usually within both the measuring range of the LISST and the grain size diameters present in suspension. Droppo & Ongley (1992, 1994) reported floc sizes in six Canadian creeks between 2 and 340 µm. Woodward et al. (2002) found floc sizes between 10 and 110 µm in glacial meltwater streams of Unteraargletscher (Switzerland) and Batura and Passu glaciers (Pakistan). Guo & He (2011) measured floc sizes between 22 and 182 µm in the Yangtze river and between 50 and 120 µm in the Yangtze estuary. If flocs were present, then they would alter the particle size distribution (Mikkelsen & Pejrup 2000) and reduce the density to values as low as 1600 kg/m^3 (Curran et al.

2007), 1370 kg/m^3 (Sassi et al 2012) or 1240 kg/m^3 (Czuba et al. 2015). Effects of organic material such as biofouling were neglected, as they are likely of minor importance because of the proximity to the glacier and its bare forefield and high elevation, combined with very cold water temperatures. Effects of mica on particle size distribution due to their platy shape were neglected as well, as there was no evidence for a significant influence based on water sample analysis.

2.2.3 ADCP measurements

Acoustic Doppler current profiler (ADCP) measurements were carried out with a SonTek RiverSurveyor M9. This 9 beam device operates with frequencies of 3 and 1 MHz, depending on the water depth, and a vertical beam echo-sounder at 0.5 MHz. The M9 device switches the frequency and adjusts the cell size depending on flow depth and velocity. The frequency of 3 MHz is used either if (a) flow depths are smaller than 1.5 m and flow velocities are lower than 0.4 m/s or (b) flow depths are smaller than 5.0 m and flow velocities are higher than 0.4 m/s (SonTek 2017). Otherwise, the frequency of 1 MHz is used. The device uses only one frequency for a specific profile, i.e. the two frequencies are never applied at the same time. Coupled to a D-GPS (accuracy < 1 m in horizontal position), the device was mounted on a hydro board attached to a boat and operated in moving real-time mode. ADCP was used to measure transects across the lake. Depth ranges under optimized conditions are 0.2 to 40 m for velocity measurements and 80 m for depth measurements. Depth ranges are, amongst other parameters, a function of SSC. Depth range was limited to approximately 30 m because at larger depths signal losses were too high under the given conditions. Measuring parameters are: (i) flow velocities; (ii) Signal-to-Noise ratios (SNR) along the water column; and (iii) depth. Flow velocity measurements have a relative accuracy of up to ±0.25% of the measured velocity and an absolute accuracy of ±2 mm/s (SonTek 2000). SNR can be used for estimating SSC, as shown by Jay et al. (1999), Alvarez & Jones (2002), Moore (2011), Guerrero et al. (2013) and Latosinski et al. (2014). Operating principles are described in detail in Moore (2011). Kostaschuk et al. (2005) and Xu et al. (2014) successfully used ADCP data to study turbidity currents in lakes and oceans, respectively. Within the scope of this study, ADCP was mainly used to identify SSC profiles using Signal-to-Noise ratios, and to measure flow velocities. Furthermore, ADCP measurements allow to track turbidity currents, which may occur in Griessee (Bourban & Papilloud 2015).

3. Results

3.1 Water sample analysis

67 water samples from both the inflowing rivers and the reservoirs were analysed. Sampling locations correspond to locations of LISST and ADCP measurements. As it was not possible to sample and measure simultaneously with ADCP and LISST, comparisons are subjected to a certain time lag in the order of ten to thirty minutes. For the relatively steady conditions, this time lag is negligible.

3.1.1 Lac de Mauvoisin

Four water samples were taken in the inflowing river and 20 in the reservoir. The particle size distributions of these samples are shown in Figure 1. In the inflowing river, on average 3% of the suspended sediments were clay (diameters below 2 µm), 89% were silt (diameters in the range from 2 to 60 µm), and 8% were sand (diameters in the range from 60 to 2000 µm). On average, the median diameter was 13 µm. In the reservoir, on average 20% were clay, 77% of the suspended sediments were silt, and 3% were sand. On average, the median diameter was 5 µm. Average SSC was 2182 mg/l in the inflowing river and 111 mg/l in the reservoir, respectively.

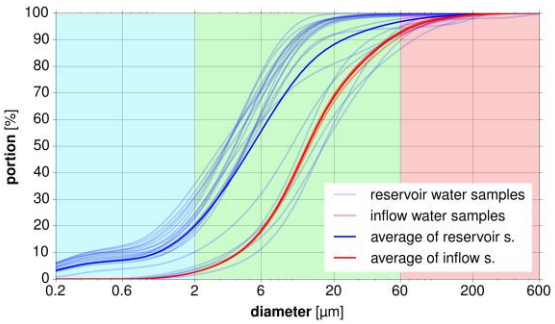

Figure 1: Particle size distribution of suspended sediments in water samples from Lac de Mauvoisin (with blue background colour for the clay, green for the silt and red for the sand fractions)

3.1.2 Griessee

On 18 August 2015, three water samples were taken in the inflowing river water and six in the reservoir. The particle size distributions are shown in Figure 2. In the inflowing river, on average 3% of the suspended sediments were clay, 88% were silt, and 9% were sand. On average, the median diameter was 13 µm. In the reservoir, on average 9% were clay, 87% of the suspended sediments were silt, and 4% were sand. On average, the median diameter was 7 µm. Average SSC was 1281 mg/l in the inflowing river and 82 mg/l in the reservoir, respectively.

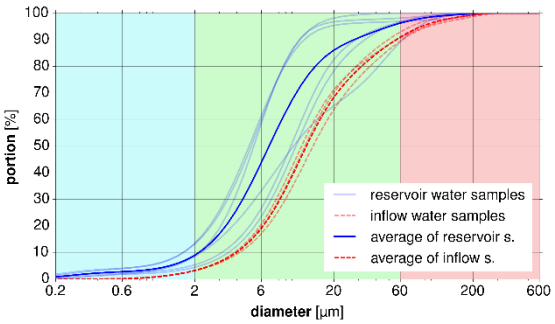

Figure 2: Particle size distribution of suspended sediments in water samples from Griessee on 18 August 2015 (with blue background colour for the clay, green for the silt and red for the sand fractions)

On 1 October 2015, eleven water samples were taken only in the reservoir because of negligible inflow. The particle size distributions are shown in Figure 3. On average, 4% were clay, 90% were silt, and 6% were sand. On average, the median diameter was 18 µm. Average SSC was 85 mg/l.

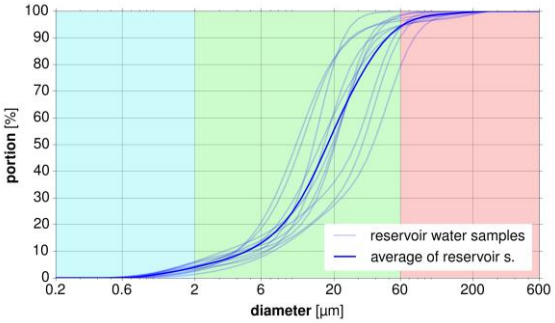

Figure 3: Particle size distribution of suspended sediments in water samples from Griessee on 1 October 2015 (with blue background colour for clay, green for silt and red for sand fractions)

On 8 August 2016, four water samples were taken in the inflowing river and 13 in the reservoir. The PSD of these samples are shown in Figure 4. In the inflowing river, on average 2% of the suspended sediments were clay, 60% were silt, and 38% were sand. The average median diameter was 37 µm. In the reservoir, on average 4% were clay, 83% of the suspended sediments were silt, and 13% were sand. The average median diameter was 19 µm. Average SSC was 4278 mg/l in the inflowing river and 122 mg/l in the reservoir, respectively.

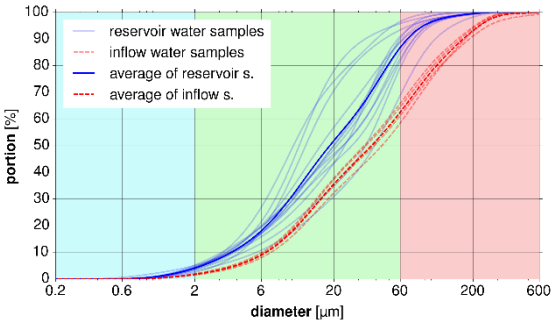

Figure 4: Particle size distribution of suspended sediments in water samples from Griessee on 8 August 2016 (with blue background colour for clay, green for silt and red for sand fractions)

3.1.3 Gebidem

On 6 October 2015, four water samples were taken in the inflowing river and 20 in the reservoir. The particle size distributions of these samples are shown in Figure 5. In the inflowing river, on average 3% of the suspended sediments were clay, 92% were silt, and 5% were sand. On average, the median diameter was 11 µm. In the reservoir, on average 4% were clay, 94% of the suspended sediments were silt, and 2% were sand. On average, the median diameter was 9 µm. Average SSC was 85 mg/l in the inflowing river and 74 mg/l in the reservoir, respectively.

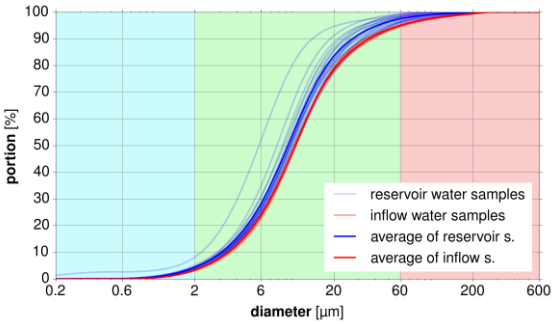

Figure 5: Particle size distribution of suspended sediments in water samples from Gebidem on 6 October 2015 (with blue background colour for clay, green for silt and red for sand fractions)

3.2 LISST measurements

3.2.1 Lac de Mauvoisin

LISST profiles over the entire reservoir depth of up to 114 m were recorded in four different locations (Figure 6). The measurement of profile L2231628 was aborted at a depth of 85 m, because either the boat or the LISST began to drift from one another due to strong currents. Median diameters were generally between 4 and 67 µm (Figure 7a). The fluctuations were high. A weak trend towards larger d50 with increasing depth could be observed. In the uppermost 20 m of the profiles, median diameters were more uniform in the order of 10 µm.

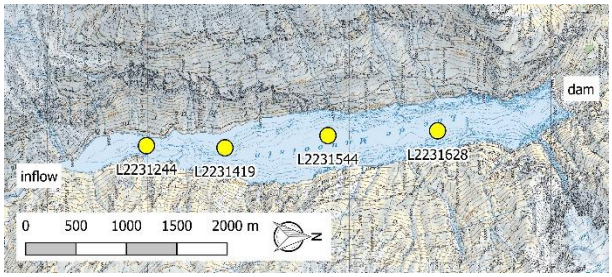

Figure 6: Location of LISST profiles in Lac de Mauvoisin [1]

SSC measurements showed a distinct increase with depth (Figure 7b). Measurements range from 39 to 2329 mg/l. In profile L2231419, the increase in SSC close to the ground is remarkably high. Either it might be because of a muddy pool or because the measuring device hit the ground and thereby swirled up the deposited fine sediments. Due to operation in logging mode, such irregularities could not be observed during the measurements and therefore no additional measurements were conducted to further examine this issue. At a depth of 80 m, transmission values decrease from 0.7 to 0.4. These values are still within the recommended application ranges, i.e. a malfunction of the instrument is unlikely.

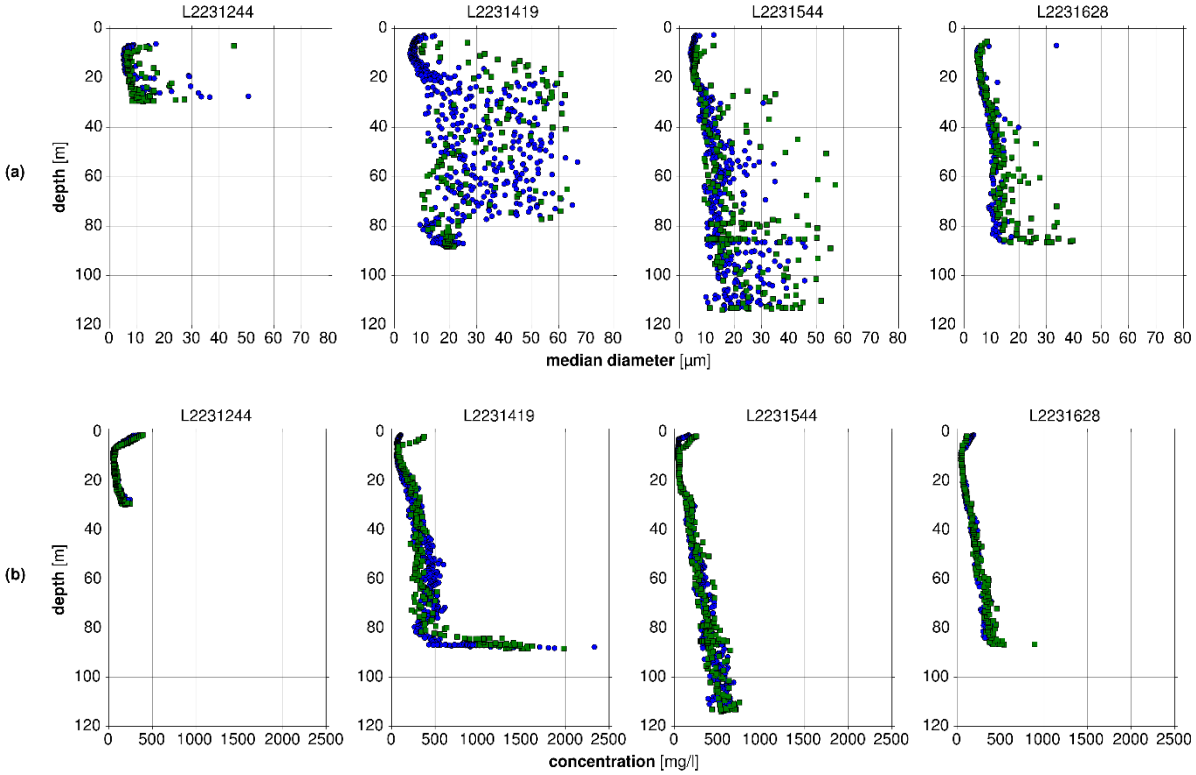

Figure 7: (a) Median diameters and (b) suspended sediment concentrations measured with LISST in Lac de Mauvoisin (blue dots indicate measurement taken while lowering the instrument, green squares indicate measurements taken while lifting the instrument)

[1] all topographical maps reproduced by permission of swisstopo (JA100120)

Figure 8 shows PSD derived from the LISST measurements. PSD have been divided into measurements from the top 20 m of the water column and measurements at larger depths. This allows an easier comparison with the water samples, which were only taken in the top 20 m. In the top 20 m (Figure 8a), median diameters are in the range of 4 to 60 µm. Measurements at larger depths (Figure 8b) have median diameters of 4 to 67 µm. Some measurements in the top 20 m show a kind of "plateau" with relatively flat PSD before it increases again. The latter increase may be attributed to the formation of flocs or influence of ambient light. As this plateau is only present in near-surface measurements, it is more likely linked to ambient light, as flocculation is expected to occur at larger depths as well. Most of the particle diameters are in the range of silt and fine sand and therefore within the measuring range of the applied LISST device.

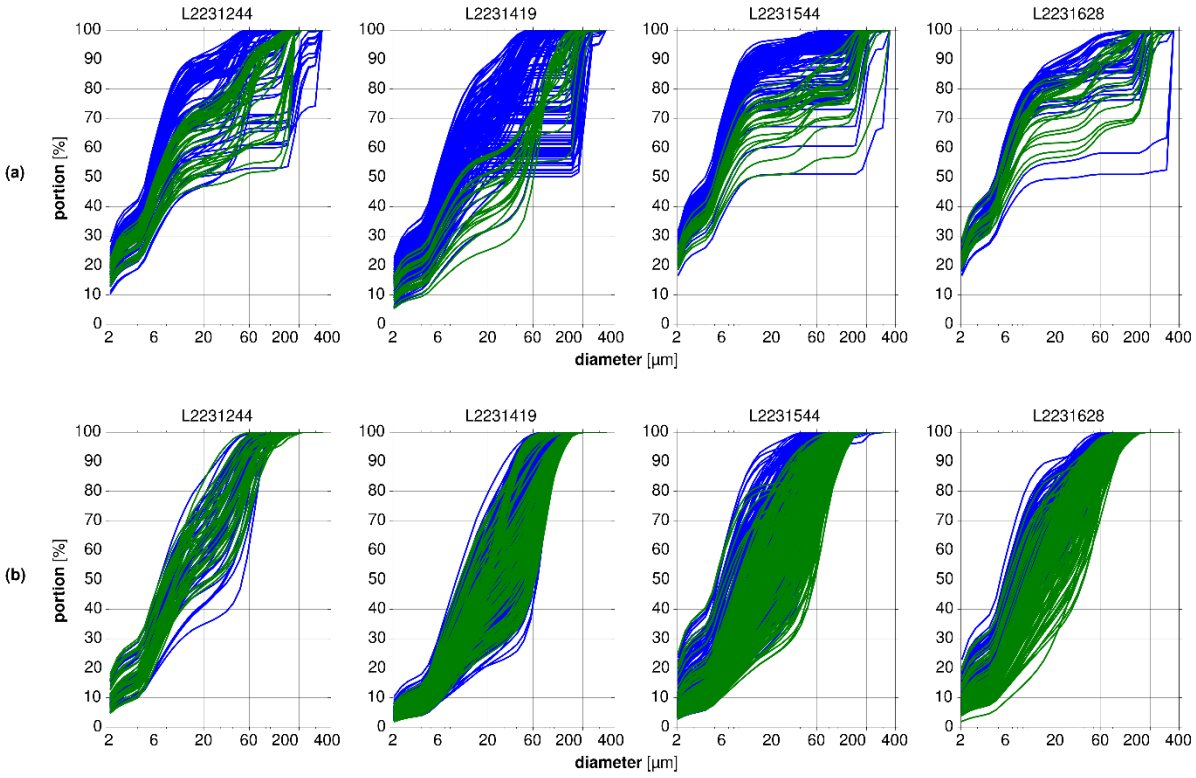

Figure 8: (a) Particle size distribution (PSD) in the top 20 m of the water column and (b) at larger depths measured with LISST in Lac de Mauvoisin (blue lines indicate measurement taken while lowering the instrument, green lines indicate measurements taken while lifting the instrument)

3.2.2 Griessee

Twelve LISST profiles were recorded in Griessee at various dates (Figure 9).

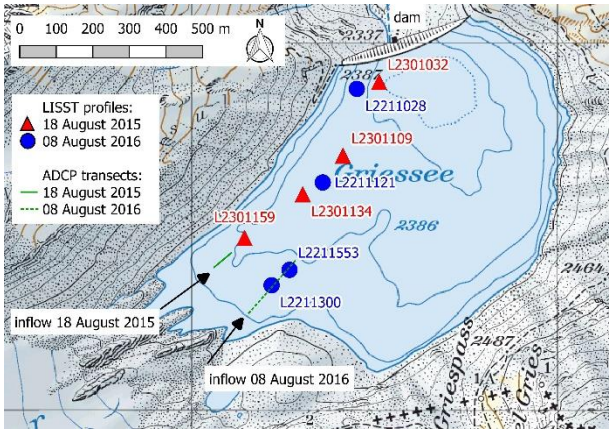

Figure 9: Location of LISST profiles and ADCP transects in Griessee

On 18 August 2015, median diameters were almost constant over the reservoir depth (Figure 10a). There are only few isolated outliers. Most measuring points showed a median diameter of about 10 µm, but values from 7 to 64 µm were recorded. SSC did not show a significant increase over depth (Figure 10b). All measured values are in the range of 60 to 248 mg/l.

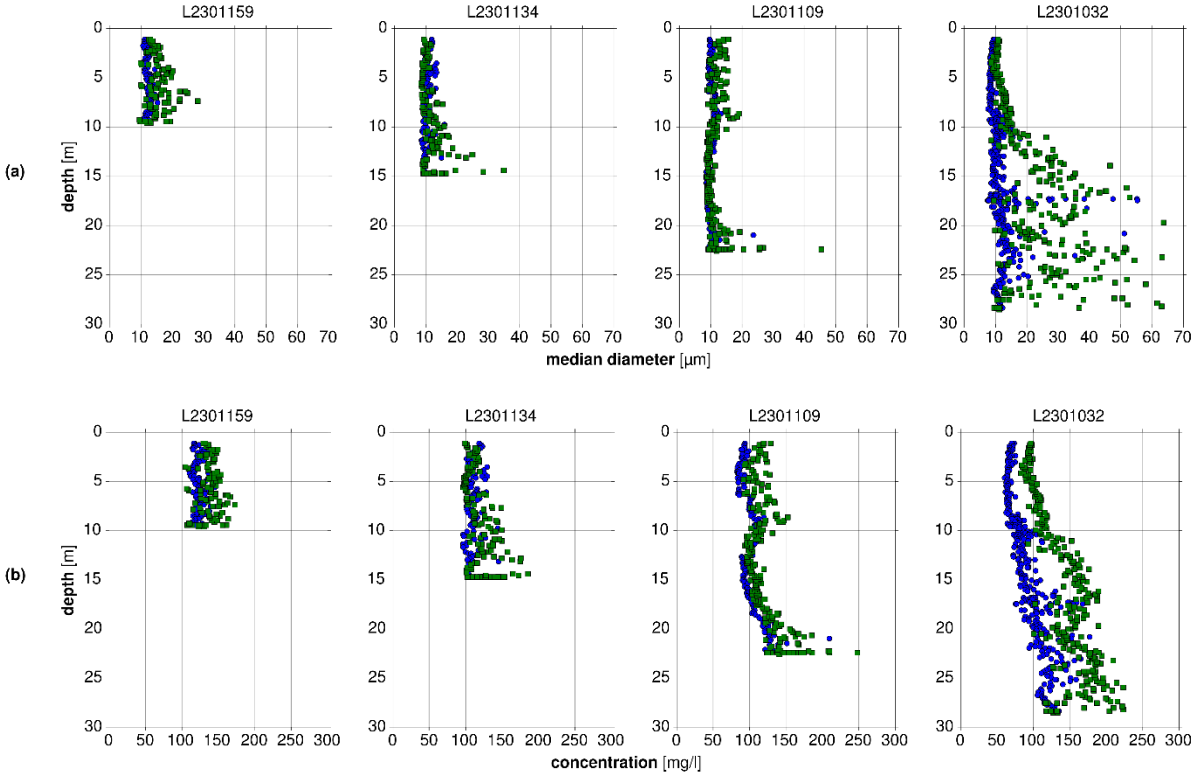

Figure 10: (a) median diameters and (b) suspended sediment concentrations measured with LISST in Griessee on 18 August 2015 (blue dots indicate measurement taken while lowering the instrument, green squares indicate measurements taken while lifting the instrument)

Figure 11 shows PSD derived from LISST measurements in the uppermost 20 m of the water column. PSD at larger depths, which were reached in two profiles only, are not shown. Most of the particles are in the range of silt and fine sand and therefore in the measuring range of the applied LISST device.

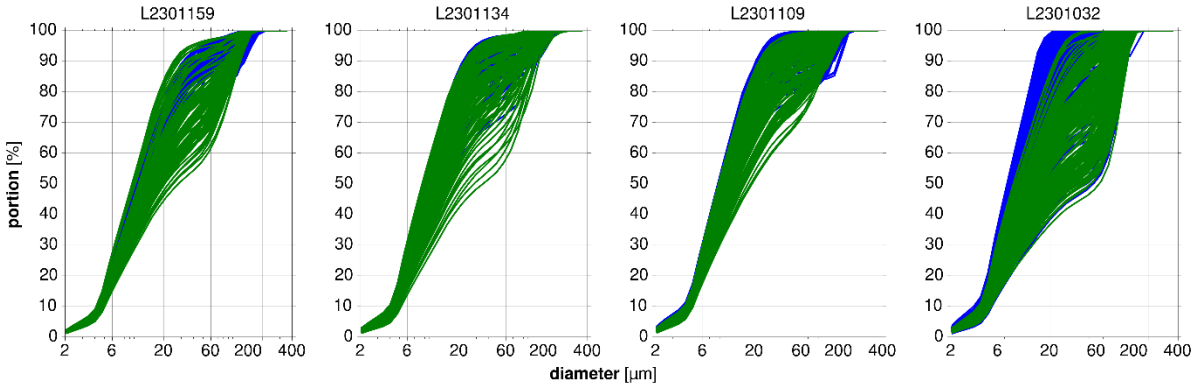

Figure 11: PSD in the uppermost 20 m of the water column measured with LISST in Griessee on 18 August 2015 (blue lines indicate measurement taken while lowering the instrument, green lines indicate measurements taken while lifting the instrument)

Due to negligible inflow, the LISST profiles of 1 October 2015 are not presented here. On 8 August 2016, a day with high peak discharge and turbid inflow, median diameters between 6 and 87 µm were recorded (Figure 12a). The trend shows an increase of the median diameters with depth. Some measurements were conducted in a stationary mode at a certain depth for at least 30 seconds. These measurements show the fluctuations of both median diameter and SSC. For example, in L2211121 at 10 m depth, the median diameters varied within one

order of magnitude between 8 and 67 µm. The fluctuations in SSC are high as well, they varied between 180 and 790 mg/l at the same depth. Similar fluctuations can be observed in other depths and profiles. Most SSC measurements are in the range of 200 to 1000 mg/l. There is a general trend towards increasing SSC with depth (Figure 12b), especially in profile L2211300, where SSC from 145 to 3008 mg/l were measured. This profile is close to the inflow, where ADCP measurements indicated evidence of a minor turbidity current. Water temperature was 6.2°C at the water surface. It decreased linearly to 6.0°C at 5 m depth and increased linearly again to peak with 6.4°C at a depth of 15 m. Optical transmission started to decrease at 10 m depth from an almost constant value of 0.7 to 0.4 at 15 m depth and decreased further to 0.2 at 17 m depth. Below a depth of 15 m, the LISST reaches its recommended application range. The decrease of SSC in L2211121 and L2211028 at depths of ca. 20 m and 15 m, respectively, can currently not be explained.

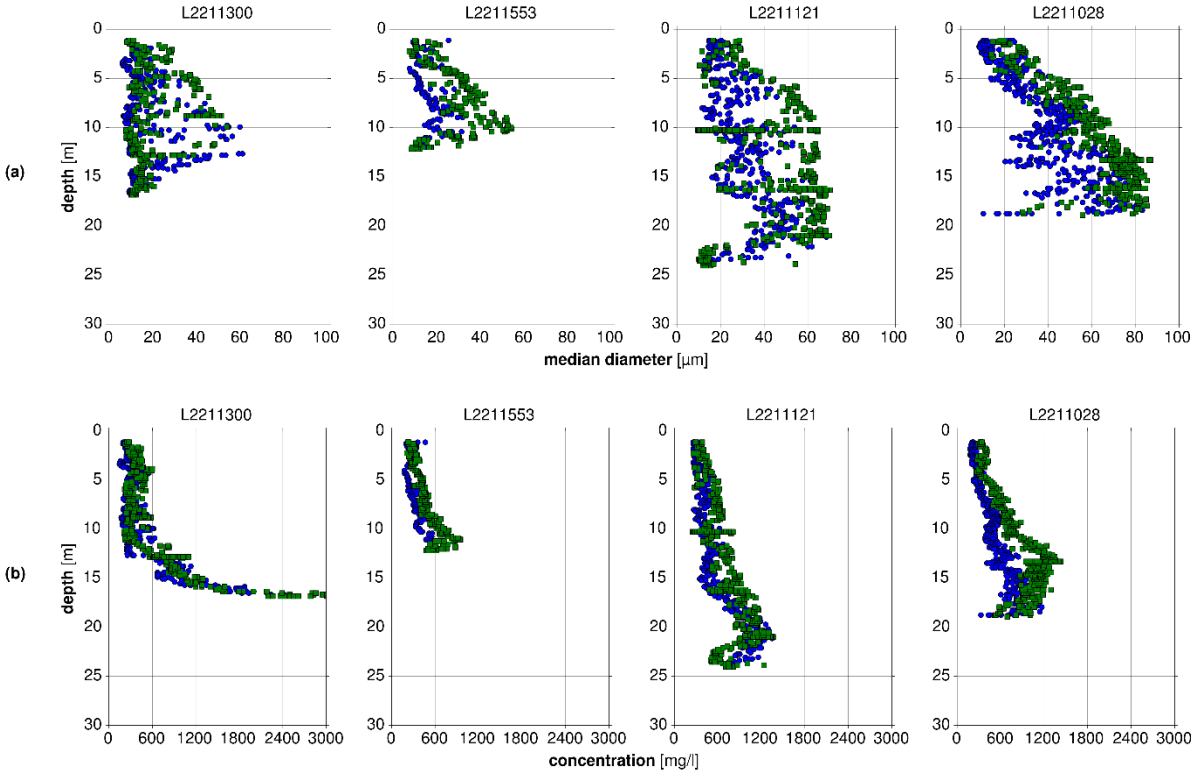

Figure 12: (a) Median diameters and (b) suspended sediment concentrations measured with LISST in Griessee on 8 August 2016 (blue dots indicate measurement taken while lowering the instrument, green squares indicate measurements taken while lifting the instrument)

PSD is shown in Figure 13 for measurements in the top 20 m of the water column (the measuring points at larger depth in profile L2211121 are not shown). Again, most particles are in the range of silt and fine sand. The plateau found in LISST measurements at Lac de Mauvoisin (Figure 8a) can equally be found in a few near-surface measurements at Griessee.

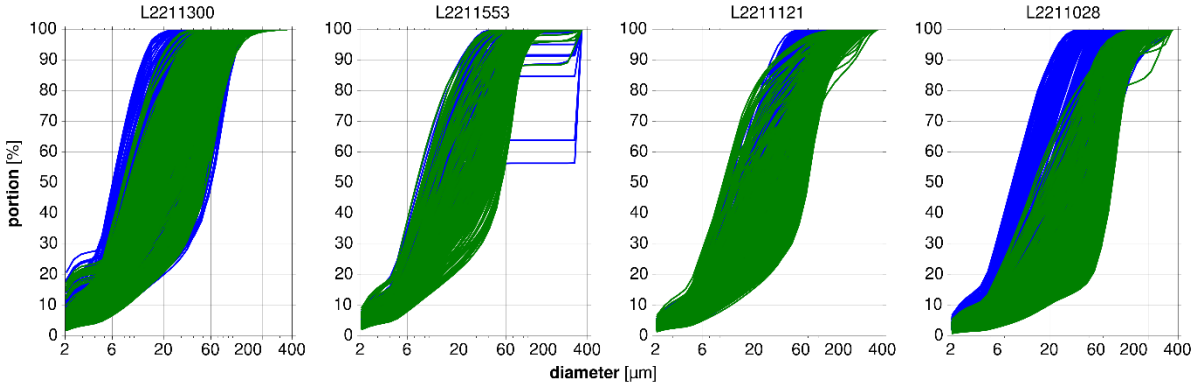

Figure 13: PSD in the top 20 m of the water column measured with LISST in Griessee on 8 August 2016 (blue lines indicate measurement taken while lowering the instrument, green lines indicate measurements taken while lifting the instrument)

3.2.3 Gebidem

Four LISST profiles were recorded in Gebidem on 6 October 2015 (Figure 14).

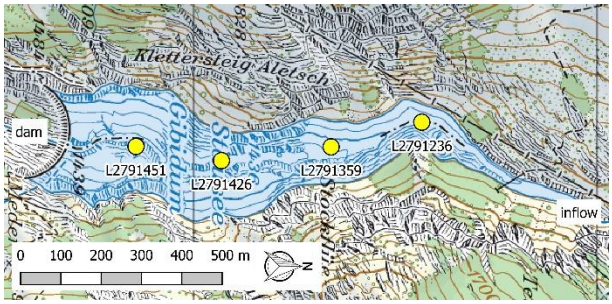

Figure 14: Location of LISST profiles in Gebidem

Median diameter were recorded between 7 and 24 µm (Figure 15a) and did not change with depth. The measurements taken while lowering the instrument differ from those taken while lifting it up. This issue appears more pronounced in the SSC records (Figure 15b). The records in the "lowering" set indicate a slight increase in SSC, but the records in the "lifting" set tend to a constant distribution of SSC over depth. No satisfying answer for this feature could be found so far. SSC measurements were in the range of 122 to 1795 mg/l. There is high scatter in the first profile L2791236, possibly because of the proximity to the inflow and its location in a curve. Both facts might lead to higher turbulent fluctuations than in the rest of the reservoir. Other reasons for the fluctuations could be organic content in the water or air bubbles, although neither were actually visible. Temperature in the first profile was 1.8°C at the surface, increased to 1.95°C in 5 m depth, and remained constant with increasing depth. In all other profiles, water temperature in the top 20 m was constantly 1.95°C. At a depth of 20 m, temperature started to decrease until a depth of 50 m, where it stayed constant again at 1.5°C. Gebidem was the only reservoir in this measuring campaign where the temperature changed over depth along the entire reservoir.

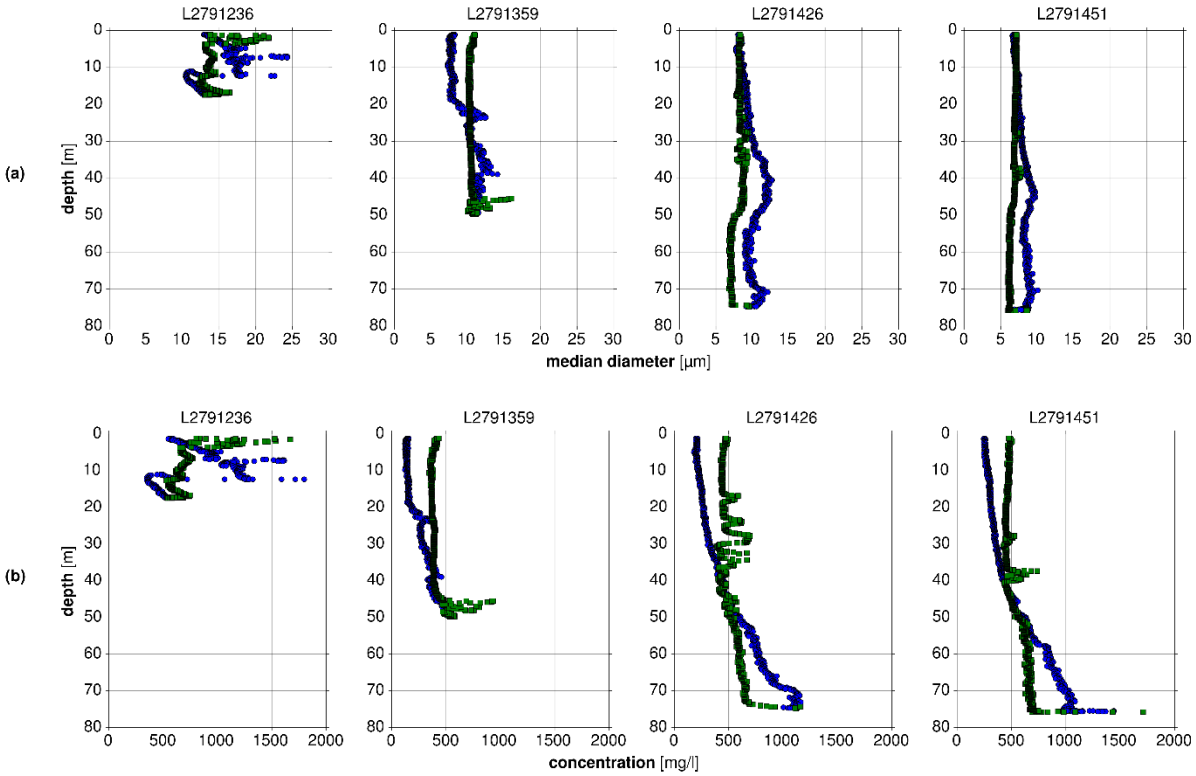

Figure 15: (a) Median diameters and (b) SSC measured with LISST in Gebidem (blue dots indicate measurement taken while lowering the instrument, green squares indicate measurements taken while lifting the instrument)

Figure 16 shows PSD derived from LISST measurements. The range of diameters is narrow, as almost all particles are in the range of silt and find sand. There is no significant difference between measurements in the top 20 m of the water column (Figure 16a) and the measurements at larger depths (Figure 16b).

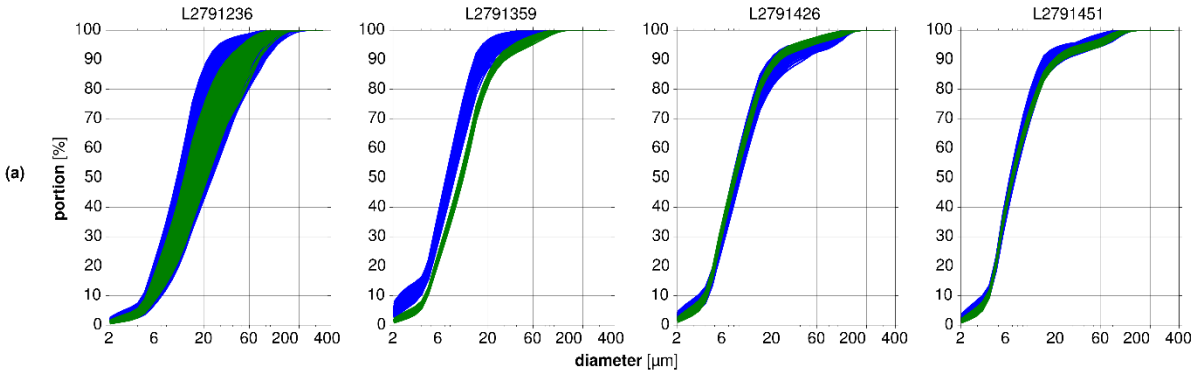

(b)

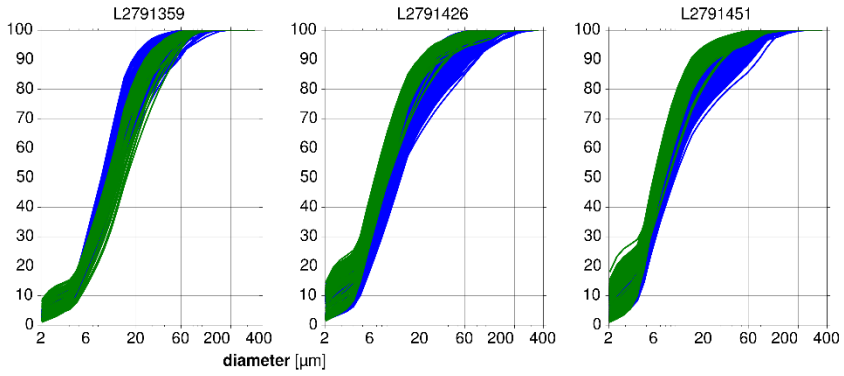

Figure 16: (a) Particle size distribution (PSD) in the top 20 m of the water column and (b) at larger depths measured with LISST in Gebidem (blue lines indicate measurement taken while lowering the instrument, green lines indicate measurements taken while lifting the instrument). N.B. that profile L2791236 was only 20 m deep.

3.3 ADCP measurements at Griessee

Various transects along and transversal to the main flow path were recorded in Griessee. Two distinct ADCP transects (Figure 9) are discussed below. Both were recorded along the flow path from the inflow to the dam. The goal was to track the distribution of the suspended sediments being conveyed into the lake. SNR values and flow velocities were the main measuring parameters.

The first 70 m long transect was recorded on 18 August 2015 (Figure 9). It can be observed that the cell size is being adjusted with increasing flow depth: at low flow depths near the inflow, cell sizes are 6 cm, whereas they are 20 cm at larger flow depths. SNR values varied between 1 and 70 dB. In general, SNR values decrease with depth (Figure 17). Close to the inflow, SNR values increase again close to the reservoir bottom. This can be observed within the first 30 m from the inflow. At higher distances from the inflow, near-surface SNR values (i.e. at the uppermost measuring point of the ADCP) varied between 20 and 40 dB. Flow velocity magnitudes varied between 0.013 m/s and 1.194 m/s with an average value of 0.164 m/s (Figure 18). Upward flow velocity magnitudes varied between -0.260 m/s and 0.264 m/s with an average value of -0.020 m/s. The average bottom slope of the transect is 5%.

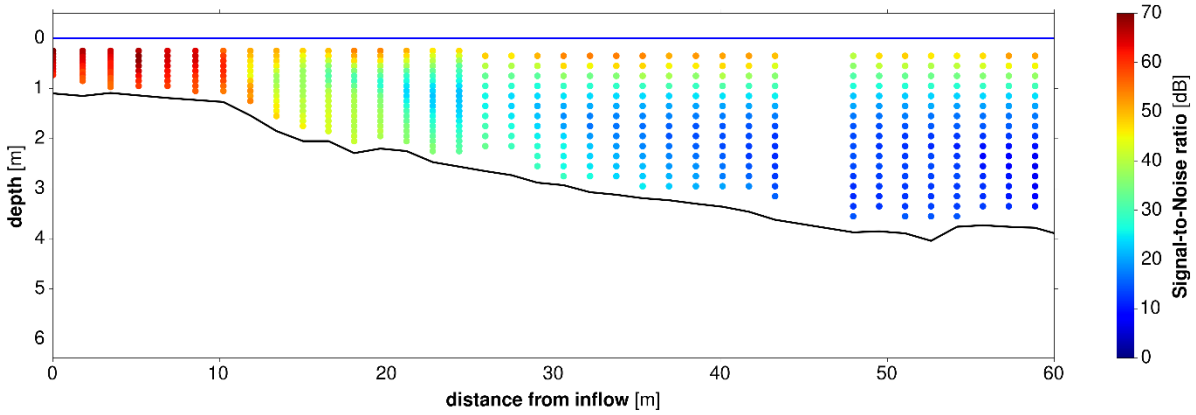

Figure 17: SNR values recorded with ADCP in a transect along the flow path on 18 August 2015 (flow direction from left to right) [2]

[2] only velocities and SNR values outside of the blanking zone and the top estimate are used in this study

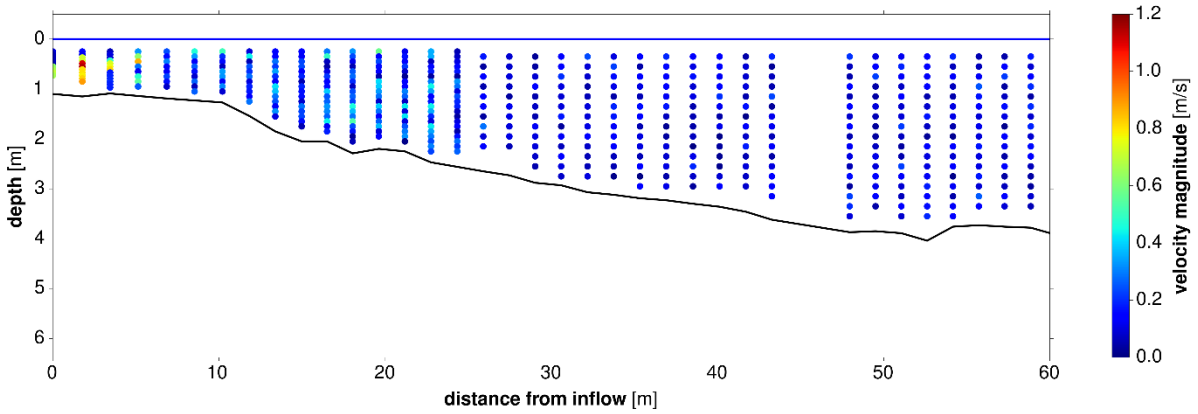

Figure 18: Flow velocity magnitudes recorded with ADCP in a transect along the flow path on 18 August 2015 (flow direction from left to right)

The second, 200 m long transect was recorded on 8 August 2016 (Figure 9). SNR values varied between 4 dB and 54 dB (Figure 19). Increasing SNR values close to the reservoir bottom could be observed within 70 m from the inflow. At larger distances from the inflow, near-surface SNR values were in the range of 25 to 35 dB. Flow velocity magnitudes varied between 0.004 m/s and 0.692 m/s with an average value of 0.138 m/s (Figure 20). Upward flow velocity magnitudes varied between -0.198 m/s and 0.145 m/s with an average value of -0.005 m/s. The average bottom slope of the transect is 6%.

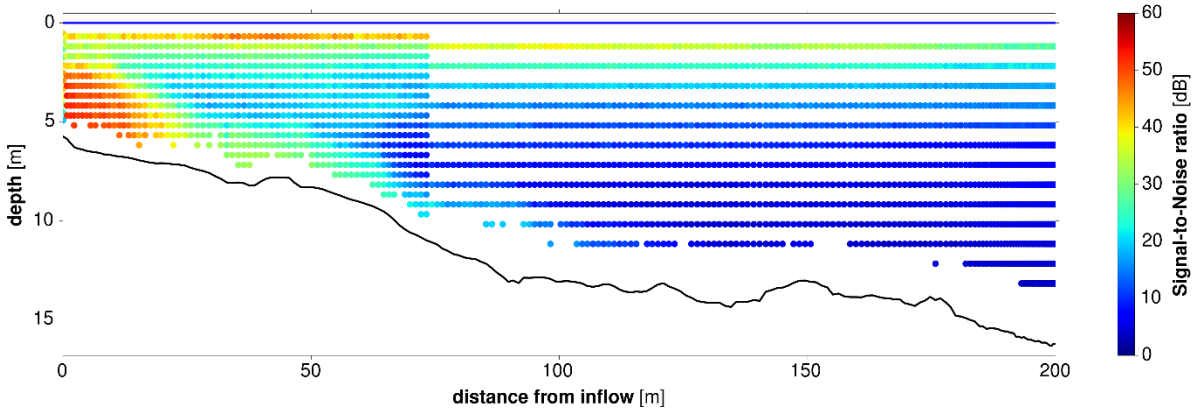

Figure 19: SNR values recorded with ADCP in a transect along the flow path on 8 August 2016 (flow direction from left to right)

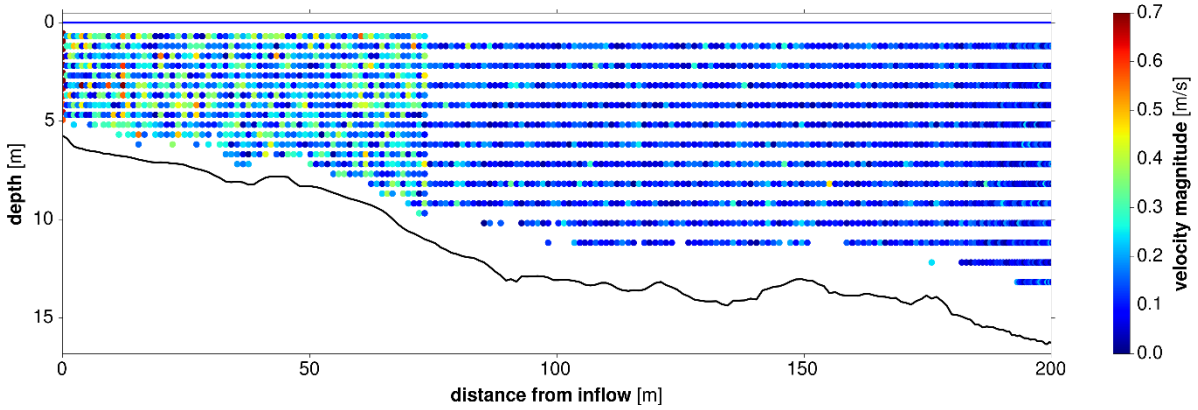

Figure 20: Flow velocity magnitudes recorded with ADCP in a transect along the flow path on 8 August 2016 (flow direction from left to right)

4. Discussion

4.1 Water sample analysis

Water sample analysis showed that 77 to 94% of the suspended sediments are within the silt fraction in all reservoirs monitored. Clay is of minor importance, and sand is probably being transported primarily as bed load. In the reservoirs, no significant spatial change of PSD was measured. PSD was slightly finer compared to the inflowing river water. Median diameters were in the range of 5 to 18 µm on average. The largest diameters were in the order of 100 µm. The settling velocity of such large particles can be calculated using Stoke's law (Eq. 1):

$$v = \frac{2}{9}\frac{\rho_p - \rho_f}{\lambda} g r^2 \quad (1)$$

where v = settling velocity of a single particle [m/s]; ρ_p = mass density of the particle [2650 kg/m^3]; ρ_f = mass density of the fluid [1000 kg/m^3]; λ = dynamic viscosity of the fluid [0.0014 kg/(m·s)]; g = gravitational acceleration [9.81 m/s^2]; and r = particle radius [m]. A particle with 50 µm radius has a settling velocity of 6.4 mm/s. Particles of that size were found close to the dam, near the water surface. They stay in suspension because turbulence is counter-acting the gravitation-driven settling process. Therefore, the effects of turbulence can be estimated: average vertical velocity fluctuations are expected to be in the range of some mm/s. This agrees well with observations reported by Hutter et al. (2011) for lakes and by Ortmanns (2006) for desanding facilities.

SSC in the inflowing water amounted up to a few g/l in summer (Lac de Mauvoisin, Griessee on 18 August 2015). In the reservoirs, SSC was in the range of 74 to 111 mg/l.

Water samples possibly provide the most reliable data source. Their acquisition and analysis in the laboratory is time-consuming and work-intensive, so that they are neither suitable for a spatially nor temporally highly resolved data set. Nevertheless, they are important for the validation of both LISST and ADCP. Although sampling depths are generally not limited, water sampling depth was herein limited to ca. 20 m due to practical limitations (manual operation of a small device from a rowing boat). Future measuring campaigns should try to overcome this issue. The positioning of the samples is another issue, because only the boat position at the water surface and the distance of the Niskin bottle sampler to the boat are known exactly. Flow velocities in the reservoir were low, so that it can be assumed that the Niskin bottle was below the boat, i.e. it had the same horizontal position and a vertical position equal to the position of the boat minus the distance between boat and Niskin bottle.

4.2 LISST measurements

Out-of-range particles mainly affect the signals in the outmost ring detectors. If significant out-of-range particles are present, these detectors are often omitted in the post-processing. Herein, no significant difference was observed if the first lower and upper three ring detectors were excluded. This is an indication that there were only little out-of-range particles (if at all), which only had minor influence on the LISST measurements. Because of the low SSC, multiple scattering was not an issue in this study.

Characteristic diameters such as median or mean could be derived from the LISST records. Different definitions of mean diameter are available, e.g. arithmetic mean, volume/surface mean (Sauter mean), mean diameter over volume (de Broukere mean) and others. This makes comparison difficult. The definition of the median was used to circumvent these problems. PSD were derived to compare LISST results with water sample results.

Some LISST records close to the surface at Lac de Mauvoisin (Figure 8a) and Griessee on 8 August 2016 (Figure 13) indicate a kind of "plateau" in the range of ca. 20 and 200 µm. This might be either due to ambient light or due to flocculation. As this feature was not observed at larger depths (Figures 8b), it is more likely linked to ambient light. Both measuring series were recorded at days with clear sky, whereas the other series (Griessee on 18 August 2015, Figure 16a, and Gebidem on 6 October 2015, Figure 11) were recorded when it was cloudy. This supports the hypothesis that the ambient light had an influence on these records.

Median diameters and PSD measured with LISST were in good agreement with water sample analysis: in the uppermost 20 m, the LISST measurements of Lac de Mauvoisin, Griessee on 18 August 2015 and Gebidem indicate median diameters in the order of 10 µm, similar to the water samples. SSC in the uppermost 20 m measured with LISST corresponds well with data from water sample analysis. The LISST measurements are in

the same order of magnitude as the water samples with 64 (minimum measured SSC) to 194 mg/l (maximum measured SSC).

The path reduction module (PRM) was applied in all measurements in 2015. Because of the 90%-PRM and the relatively low SSC, optical transmission values were generally high, i.e. above 0.8. Nevertheless, the results are generally in good agreement with water sample analysis. No negative effect of the PRM could be observed in the measuring data. Measurements in 2016 were taken without PRM. They have lower optical transmission values between 0.4 and 0.7.

Haun et al. (2015) compared results gained with LISST-SL and LISST-STX in stationary mode to those from moving (where the device was kept at a pre-defined depth and moved horizontally) operation mode 3 and measured distinct differences in SSC (up to 9%) and in median diameters (up to 19%). Therefore, the operation mode may affect the measurement results. In Griessee on 8 August 2016, both stationary and moving measurements were recorded. Here, moving mode refers to lowering and lifting the instrument at a fixed location. Furthermore, a slightly different type of device was applied, so the results are not directly comparable. Median diameters varied by a factor of 10, SSC varied by a factor of 5. It is impossible to distinguish between the influence of the operating mode (stationary/moving) and natural fluctuations possibly caused by turbulence. The average of each stationary measurement is in line with the value measured in moving operation mode (e.g. Figure 12a, profile L2211121). Felix et al. (2013) reported the ratio of instantaneous SSC and time-averaged SSC in a laboratory analysis. The ratio was generally between 1.5 and 0.5, i.e. much lower than the fluctuations observed herein. It can consequently be assumed that the fluctuations are mainly caused by natural variability and not by the operation mode.

LISST measurements are valuable, as they provide PSD and SSC simultaneously ~~independently~~. Easy handling and straight-forward data processing are advantages of this technique. LISST can be operated in real-time mode, which allows identifying irregularities in the water body where water samples should be taken. Major drawbacks are the limited range of PSD and SSC. The depth of each record is known exactly as the pressure is measured by the instrument. The horizontal position cannot be measured, but it can be assumed to be equal to the boat position, given the low flow velocities in the reservoir.

4.3 ADCP measurements

It is not possible to derive PSD from a single frequency ADCP. Guerrero et al. (2011) showed that the combination of at least two ADCPs working on different frequencies is needed to derive PSD.

SSC can be derived from the Signal-to-Noise ratio (SNR). Various approaches are provided in literature. The most basic formulations link SNR directly with SSC. Thevenot et al. (1992) proposed the following formula (Eq. 2):

$$SSC = 10^{A+B \cdot SNR_{corr}} \quad (2)$$

where SSC = suspended sediments concentration [mg/l]; A = calibration parameter [–]; B = calibration parameter [–]; and SNR_{corr} = Signal-to-Noise ratio [dB] corrected for transmission losses. If the signal propagation distance is small, transmission losses can be neglected. This is true for near-surface measurements. Alvarez & Jones (2002) derived a linear correlation between SSC gained from water sample analysis and SNR from measurements with a SonTek ADP. They found coefficient A = 1.1186 and B = 0.0245. In the Griessee reservoir, SNR values close to the surface varied between 20 and 40 dB. Applying the coefficients of Alvarez & Jones (2002), this would lead to SSC of 41 to 125 mg/l. This is in good agreement with the data from water sample analysis and LISST measurements. The higher SNR values of 50 to 70 dB close to the inflow would lead to SCC of 221 to 682 mg/l if Alvarez' & Jones' (2002) coefficients were applied. This is supported by two water samples from the reservoir inflow region that had SSC of 151 and 274 mg/l, while the inflowing river water had SSC of 1300 mg/l. The SNR values may consequently be used for the determination of SSC using Eq. (2). Given the small amount of water samples suitable to derive a correlation of SSC and SNR and the fact that the relationship of Alvarez & Jones (2002) provided satisfactory results, no attempt was made to carry out a new regression analysis.

[3] in stationary operation mode, the device is kept at a fixed depth at a certain location; in moving operation mode, depth or location change

SNR obtained in larger depths can be used to determine SSC as well. These SNR data need to be corrected for three types of transmission losses: (i) beam spreading; (ii) absorption by water; and (iii) absorption by sediment. Urick (1975) presented the SONAR equation, which accounts for these 3 types of transmission losses. Wood & Gartner (2010) derived the following form of the SONAR equation suitable for SonTek ADCP measurement (Eq. 3):

$$SNR_{corr} = SNR + 20log_{10}R + 2\alpha_W R + 2\alpha_S R \quad (3)$$

where SNR_{corr} = corrected SNR [dB]; SNR = measured SNR [dB]; R = distance [m]; α_W = absorption coefficient of water [dB/m]; and α_S = absorption coefficient of sediment [dB/m]. These corrected SNR values can be used to derive SSC. Moore (2011) presents a procedure to calculate α_W and α_S. The former depends on water temperature and ADCP frequency, the latter on ADCP frequency, density of water and sediment, sound speed in water, particle radius, and SSC itself. In general, α_S has to be determined with an empirical or statistical relationship, as e.g. proposed by Wood & Teasdale (2013). It changes with PSD and SSC. Absorption of sediment can be further divided into absorption due to scattering attenuation and viscous attenuation.

Small particles and low SSC lead to small values of α_S. Figure 21 shows the three types of transmission losses for a case using the following values: ADCP frequency = 1 MHz, water temperature = 6°C, sound speed in water = 1500 m/s, density of water and sediment = 1000 kg/m^3 and 2650 kg/m^3, respectively, particle radius r = 20 µm, and SSC = 100 mg/l. Such values are similar to those found in the investigated reservoirs of this study. Most of the transmission loss is caused by beam spreading. Absorption by water is one order of magnitude smaller. Absorption by sediment is another order of magnitude smaller. Basically, transmission losses due to absorption by sediment can be neglected for the small particles and relatively low SSC. For the chosen values, scattering attenuation is 1.4% of the total absorption of sediment, whereas viscous attenuation amounts to 98.6%.

Adjustments due to transmission losses should exceed the noise level. This might not necessarily be the case for absorption by sediment. If so, SSC could not be derived from SNR values alone. Nevertheless, ADCP measurements are valuable to identify and to track density currents, since propagation distance and current height can be estimated. Low ADCP frequencies would be preferable as they reduce the backscatter from large particles and increase the attenuation of clay and silt (Guerrero et al. 2016). It is not clear how flocs would affect ADCP measurements (Moate & Thorne 2009).

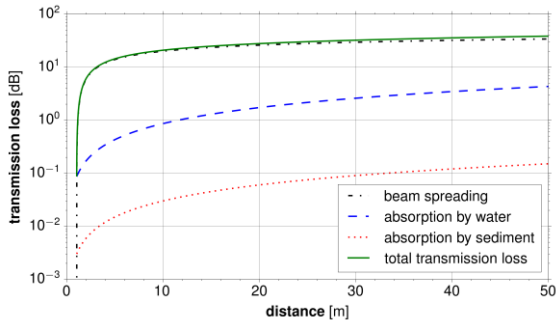

Figure 21: Transmission losses according to the procedure presented in Moore (2011). The calculations where done for a frequency of 1 MHz, a water temperature of 6°C, speed of sound in water of 1500 m/s, water and sediment densities of 1000 kg/m^3 and 2650 kg/m^3, respectively, a particle radius of 20 µm, and SSC of 100 mg/l

On 18 August 2015, increasing SNR towards the reservoir bottom could be detected up to a distance of ca. 30 m from the inflow (Figure 17). On 8 August 2016, increasing SNR were detected up to a distance of ca. 70 m (Figure 20). These increases can be interpreted as minor turbidity currents. The propagation distance is small and the turbidity currents decay within some dozens of meters from the inflow because the density difference between inflowing river water and reservoir water is no longer large enough to maintain these density-driven currents. Decaying turbidity currents deposit sediments, i.e. bathymetric measurements conducted in autumn 2016 where analysed as to corresponding deposition patterns (Delaney et al. 2016). The turbidity currents were not distinct, i.e. there was no clear boundary between plunging inflowing river water and ambient reservoir water. LISST profile L2211300 (Figure 12b), located in the inflow region, shows a distinct increase in SSC close to the reservoir bottom. This is an additional evidence of an existing turbidity current. The moderate increase of water temperature further indicates the existence of such a current. This was expected, as there is hardly any temperature difference between inflowing river water and the reservoir.

ADCP measurements provide unique advantages: they are non-intrusive, have a high degree of spatial and temporal resolution and allow profile measurements, where flow velocities at different depths are measured simultaneously. SNR, a by-product, can be used for SSC estimations. Data acquisition is cheap in terms of time and work compared to other techniques. This allows to record transects all over the reservoir, i.e. a high spatial resolution. Fast data acquisition allows a high temporal resolution as well. Unfortunately, the translation from SNR to SSC remains a major issue. The actual PSD and SSC are necessary for adjusting SNR for transmission losses. Iterative calibration techniques are available, but their application range is limited. Using water samples is the best way to calibrate the ADCP data. Taking calibration samples simultaneously to ADCP measurements is hardly possible, however.

5. Summary and conclusions

Reservoir sedimentation is determined by sediment conveyance into the reservoir and the sediment fluxes within the reservoir. In the periglacial environment, sediment conveyance is strongly linked with glacier evolution and is expected to change in the next decades, as glaciers will retreat due to climate change. Particle size distribution (PSD) and suspended sediment concentrations (SSC) in Swiss periglacial reservoirs have not yet been studied systematically. This study provides field data for Lac de Mauvoisin, Griessee and Gebidem, acquired with the combination of water sample analysis, LISST and ADCP.

Analysis of 85 water samples showed that 77 to 94% of the suspended sediments in the investigated reservoirs were silt. Clay portions were between 4 and 20%, sand portions were between 2 and 13%. Median diameters varied between 5 and 19 µm and average SSC was measured between 74 and 122 mg/l. Both PSD and SSC did not show significant spatial variations in the three reservoirs (Figures 1–5). Water sampling was restricted to the uppermost 20 m due to technical limitations. In the inflowing rivers, 60 to 92% of the suspended sediments were silt. Clay and sand portions ranged from 2 to 3% and 5 to 38%, respectively. Median diameters were between 11 and 37 µm. Average SSC was measured from 85 to 4278 mg/l. Water sample analysis did not show evidence of significant flocculation as probes before and after ultrasounding did not reveal different particle size distributions. Nevertheless, long storage times or drying procedures can result in cluster formation, which should not be misinterpreted as flocculation.

The 16 measurements with laser in-situ scattering and transmissometry (LISST) were in good agreement with the water sample analysis. The LISST device was able to reproduce the whole range of PSD, and characteristic diameters such as the median could be derived. At Lac de Mauvoisin, where large depths of more than 100 m were reached, a slight increase in PSD (Figure 7a) and a pronounced increase in SSC (Figure 7b) were observed. The trend of increasing SSC with depth was likewise observed in Griessee (Figure 10b and 12b), where depths were less than 30 m. A distinct trend of increasing PSD could not be detected (Figures 10a and 12a), however. In Gebidem, a deep reservoir similar to Lac de Mauvoisin, the trend of increasing SSC was only weak (Figure 15b), which may be linked to the fact that these measurements were taken late in the season and correspond to a "winter state" rather than to a "summer state" as for example in Lac de Mauvoisin. PSD was constant over the whole flow depth (Figure 15a).

PSD from LISST measurements (Figures 8, 11, 13, and 16) could be computed using all bin sizes, as hardly any out-of-range particles were present and multiple scattering was not an important factor, given the low SSC. Flocculation and the effects of mica or organic content were neglected. Flocculation could not be detected by means of LISST measurements, as the floc sizes would be in the same range as the grain sizes in suspension. Measuring flocs combined with single particles would hinder conversion from volume to mass concentration, as the density would be strongly reduced because of the flocs present. Some near-surface measurements were possibly affected by ambient light, so that all measurements at depths smaller than 1 m to the surface were neglected. An unsolved issue is the fact that measurements from moving operation mode (i.e. lowering and lifting the instrument at constant speed of 0.1 m/s at a given location) and stationary operation mode (i.e. keeping the instrument at a certain depth and location) deviate (Figure 12). Stationary measurements showed variations of up to a factor of 10 for median diameters and fluctuations of up to a factor of 5 for SSC. It is assumed that the stationary measurements reveal the natural fluctuations, but this needs to be proven with further measuring campaigns.

ADCP measurements in Griessee provided not only flow velocities, but also SNR that can be used to estimate SSC. Because of relatively low SSC, the influence of SSC on the SNR values was hardly detectable. Beam spreading and attenuation by water determined signal losses and therefore the SNR values. This is supported by

findings of Guerrero et al. (2014). ADCP measurements could not be used for reliable quantitative SSC estimates. Nevertheless, the measurements provided a qualitative view of SSC in the inflow region, as the mixing of inflowing river water with lake water can be studied. On 18 August 2015, there was evidence of a stratified flow in terms of SSC up to a distance of ca. 30 m from the inflow at Griessee. On 8 August 2016, the stratified flow reached distances of ca. 70 m from the inflow. The stratification was most likely due to the evolution of minor turbidity currents, as inflowing river water had SSC of 1281 mg/l and 4278 mg/l, whereas average SSC in the reservoir was 82 mg/l and 122 mg/l, respectively. The higher SSC on 8 August 2016 led to a stronger turbidity current with longer propagation distance and increased thickness (Figures 17 and 19). Nevertheless, the density difference was not high enough for the evolution of a distinct turbidity current, i.e. the upper boundary of the turbid layer is not distinct, and the turbidity current decays rapidly, the more so as the bottom slope is relatively mild. After a dozen of meters, the turbidity current is being mixed with ambient reservoir water and the hyperpycnal conditions change to homopycnal conditions.

Water samples provide the most robust data set. Due to their time-consuming and work-intensive acquisition, their number should be kept small. LISST provides the unique opportunity to measure both PSD and SSC, but the application range is limited. In most parts of the lake, PSD and SSC are within this range. The effort of data acquisition with LISST is between water sample analysis and ADCP measurements. ADCP measurements can be obtained with the lowest effort, but because of small particles and low SSC they provide mainly qualitative results regarding SSC. Flow velocities can be measured within the accuracy range guaranteed by the manufacturer. The chosen ADCP device was not optimal for the PSD and SSC encountered in the reservoir. It would be preferable to have an ADCP with lower frequency to (a) reach larger depths and (b) increase the portion of sediment absorption (and reduce the portion of water absorption) in the signal loss correction procedure.

The set of the three measuring techniques – water sampling, LISST and ADCP – was applied successfully to study PSD and SSC in periglacial reservoirs. Main findings are: (a) Most of the suspended sediments in the reservoir are in the range of silt and clay. Sand and gravel present in the inflow is likely being transported as bed load; (b) the median diameter does only weakly increase with depth (if at all); (c) the increase of SSC with depth is more pronounced if depth ranges are large; (d) there is no evidence of significant changes of PSD and SSC on the horizontal plane within the reservoir; (e) sediment-laden inflowing river water may lead to turbidity currents, but these stratified flows were restricted close to the inflow zones for the given reservoir; (f) in most parts of the reservoirs, homopycnal conditions seem to be dominant; (g) LISST-100X is the most suitable device to examine PSD and SSC in periglacial reservoirs because it covers the entire ranges of present PSD and SSC; (h) water sample analysis are crucial to check the plausibility of the LISST records; and (i) there is no evidence that flocculation or the influence of mica or organic content significantly influenced the LISST measurements. Ambient light has to be taken into account, however.

In a next step, these findings will be used for the calibration and validation of a numerical model to simulate reservoir sedimentation. This model will be used to forecast future evolution of reservoirs taking the changing climate and its impact on water discharge and sediment yield into account.

6. Acknowledgements

The project is financially supported by the Swiss National Science Foundation (SNSF) within the National Research Programme NRP 70 “Energy Turnaround” Project No. 153927. It is under the umbrella of the Swiss Competence Center for Energy Research – Supply of Electricity (SCCER-SoE). The field work was technically supported by Forces Motrices de Mauvoisin / Axpo, Ofima / Kraftwerk Aegina AG, Electra Massa / Alpiq and HYDRO Exploitation SA.

References

Addor, N.; Rössler, O.; Köplin, N.; Huss, M.; Weingartner, R.; Seibert, J. (2014). Robust changes and sources of uncertainty in the projected hydrological regimes of Swiss catchments. *Water Resources Research* 50(10): 7541–7562. http://dx.doi.org/10.1002/2014wr015549

Agrawal, Y. C. & Pottsmith, H. C. (1994). Laser diraction particle sizing in STRESS. *Continental Shelf Research* 14(10): 1101–1121. http://dx.doi.org/10.1016/0278-4343(94)90030-2

Agrawal, Y. C. & Pottsmith, H .C. (2000). Instruments for particle size and settling velocity observations in sediment transport. *Marine Geology* 168(1): 89–114. http://dx.doi.org/10.1016/s0025-3227(00)00044-x

Agrawal, Y. C.; Whitmire, A.; Mikkelsen, O. A.; Pottsmith, H. C. (2008). Light scattering by random shaped particles and consequences on measuring suspended sediments by laser diffraction. *Journal of Geophysical Research: Oceans* 113(C4). http://dx.doi.org/10.1029/2007jc004403

Alvarez, L. G. & Jones, S. E. (2002). Factors Influencing Suspended Sediment Flux in the Upper Gulf of California. *Estuarine, Coastal and Shelf Science* 54(4): 747–759. http://dx.doi.org/10.1006/ecss.2001.0873

Andrews, S. W.; Nover, D. M.; Reardon, K. E.; Reuter, J. E.; Schladow, S.G. (2011a). The influence of ambient light intensity on in situ laser diffractometers. *Water Resources Research* 47(6): 1–10. http://dx.doi.org/10.1029/2010wr009841.

Andrews, S. W.; Nover, D. M.; Reuter, J. E.; Schladow, S. G. (2011b). Limitations of laser diffraction for measuring fine particles in oligotrophic systems: Pitfalls and potential solutions. *Water Resources Research* 47(5): 1–12. http://dx.doi.org/10.1029/2010wr009837

Auel, C. & Boes, R.M. (2012). Sustainable reservoir management using sediment bypass tunnels. *Proc. 24th ICOLD Congress*. International Commission on Large Dams (ICOLD), Kyoto, Japan. Q.92, R.16: 224-241

Bartholomä, A.; Kubicki, A.; Badewien, T. H.; Flemming, B. W. (2009). Suspended sediment transport in the German Wadden Sea – seasonal variations and extreme events. *Ocean Dynamics* 59(2): 213–225. https://doi.org/10.1007/s10236-009-0193-6

Beck, M. & Baron, L. (2011). Bathymetrie Gries – Rapport Technique ('Bathymetry Gries – Technical Report'). *Technical Report*, R.B.R. Geophysics GmbH (unpublished)

Beck, M. & Baron, L. (2015). Bathymetrie Gries – Rapport Technique ('Bathymetry Gries – Technical Report'). *Technical Report*, R.B.R. Geophysics GmbH (unpublished)

Beyer Portner, N. (1998). Erosion des bassins versant alpins suisses par ruisellement de surface ('Erosion of alpine catchments in Switzerland by overland flow'). *PhD thesis*, Ecole Polytechnique Fédérale de Lausanne (EPFL). https://infoscience.epfl.ch/record/116153/files/Comm_LCH_6.pdf&version=1 (accessed: 25/04/2017; in French)

Bourban, G. & Papilloud, E. (2015). Gries: a global approach example for hydropower reservoir sedimentation management. *Proc. HYDRO 2015*, 1–6

CH2011 (2011). Swiss Climate Change Scenarios 2011. *Technical Report*, C2SM, MeteoSwiss, ETH, NCCR Climate and OcCC, Zürich. http://www.ch2011.ch/pdf/CH2011reportHIGH.pdf (accessed: 25/04/2017)

Curran, K. J.; Hill, P.S.; Milligan, T. G.; Mikkelsen, O. A.; Law, B. A.; de Madron, X. D.; Bourrin, F. (2007). Settling velocity, effective density, and mass composition of suspended sediment in a coastal bottom boundary layer, Gulf of Lions, France. *Continental Shelf Research* 27(10): 1408–1421. http://dx.doi.org/10.1016/j.csr.2007.01.014

Czuba, J. A.; Straub, T. D.; Curran, C. A.; Landers, M. N.; Domanski, M. M. (2015). Comparison of fluvial suspended-sediment concentrations and particle-size distributions measured with in-stream laser diffraction and in physical samples. *Water Resources Research* 51(1): 320–340. http://dx.doi.org/10.1002/2014wr015697

Delaney, I. A.; Bauder, A.; Huss, M.; Weidmann, Y. (submitted). Proglacial erosion rates and processes in a Swiss glacier's catchment. *Earth Surface Processes and Landforms*

Droppo, I. G.; Ongley, E. D. (1992). The state of suspended sediment in the freshwater fluvial environment: a method of analysis. *Water Research* 26(1): 65–72. http://dx.doi.org/10.1016/0043-1354(92)90112-h

Droppo, I. G.; Ongley, E. D. (1994). Flocculation of suspended sediment in rivers of southeastern Canada. *Water Research* 28(8): 1799–1809. http://dx.doi.org/10.1016/0043-1354(94)90253-4

Duclos, P.-A.; Lafite, R.; le Bot, S.; Rivoalen, E.; Cuvilliez, A. (2013). Dynamics of turbid plumes generated by marine aggregate dredging: An example of a macrotidal environment (the Bay of Seine, France). *Journal of Coastal Research* 29(6A): 25–37. https://doi.org/10.2112/jcoastres-d-12-00148.1

Farinotti, D.; Usselmann, S.; Huss, M.; Bauder, A.; Funk, M. (2012). Runoff evolution in the Swiss alps: projections for selected high-alpine catchments based on ENSEMBLES scenarios. *Hydrological Processes* 26(13): 1909–1924. http://dx.doi.org/10.1002/hyp.8276

Felix, D. (2017). Experimental investigation on suspended sediment, hydro-abrasive erosion and efficiency reductions of coated Pelton turbines. *PhD Thesis, VAW-Mitteilung 238*, Laboratory of Hydraulics, Hydrology and Glaciology (VAW), R. M. Boes (ed.), ETH Zürich, Switzerland (in prep.)

Felix, D.; Albayrak, I.; Boes, R. M. (2013). Laboratory investigation on measuring suspended sediment by portable laser diffractometer (LISST) focusing on particle shape. *Geo-Marine Letters* 33(6): 485–498. http://dx.doi.org/s00367-013-0343-1

Fettweis, M.; Francken, F.; Pison, V.; Van den Eynde, D. (2006). Suspended particulate matter dynamics and aggregate sizes in a high turbidity area. *Marine Geology* 235(1-4): 63–74. https://doi.org/10.1016/j.margeo.2006.10.005

Gabbi, J.; Farinotti, D.; Bauder, A.; Maurer, H. (2012). Ice volume distribution and implications on runoff projections in a glacierized catchment. *Hydrology and Earth System Sciences* 16(12): 4543–4556. http://dx.doi.org/10.5194/hess-16-4543-2012

Geilhausen, M.; Morche, D.; Otto, J.-C.; Schrott, L. (2013). Sediment discharge from the proglacial zone of a retreating alpine glacier. *Zeitschrift für Geomorphologie* 57(2): 29–53. http://dx.doi.org/10.1127/0372-8854/2012/s-00122

Guerrero, M.; Szupiany, R. N.; Amsler, M. (2011). Comparison of acoustic backscattering techniques for suspended sediments investigation. *Flow Measurement and Instrumentation* 22(5): 392–401. http://dx.doi.org/10.1016/j.flowmeasinst.2011.06.003

Guerrero, M.; Szupiany, R. N.; Latosinski, F. (2014). Multi-frequency acoustic for suspended sediment studies: an application in the Parana River. *Journal of Hydraulic Research* 51(6): 696–707. https://doi.org/10.1080/00221686.2013.849296

Guerrero, M.; Rüther, N.; Archetti, R. (2014). Comparison under controlled conditions between multi-frequency ADCPs and LISST-SL for investigating suspended sand in rivers. *Flow Measurement and Instrumentation* 37: 73–82. https://doi.org/10.1016/j.flowmeasinst.2014.03.007

Guerrero, M.; Rüther, N.; Szupiany, R.; Haun, S.; Baranya, S. Latosinski, F. (2016). The acoustic properties of suspended sediment in large rivers: Consequences on ADCP methods applicability. *Water-MDPI* 8(13): 1–22. https://doi.org/10.3390/w8010013

Guillon, H. (2016). Origine et transport des sédiments dans un bassin versant alpin englacé (Glacier des Bossons, France) ('Origin and transport of sediments in a glaciated alpine drainage basin (Glacier des Bossons, France)'). *PhD Thesis*, Université Grenoble Alpes. https://tel.archives-ouvertes.fr/tel-01461481v2/document (accessed: 25/04/2017; in French)

Guo, L.; He, Q. (2011). Freshwater flocculation of suspended sediments in the Yangtze River, China. *Ocean Dynamics* 61(2/3): 371–386. http://dx.doi.org/10.1007/s10236-011-0391-x

Gurnell, A.; Hannah, D.; Lawler, D. (1996). Suspended sediment yield from glacier basins. *Proc. Erosion and Sediment Yield: Global and Regional Perspectives*, D. E. Walling; B. Webb (eds.). International Association of Hydrological Sciences (IAHS), Exeter, England: 97–104. ISBN 9780947571894.

Ha, H. K.; Kim, Y. H.; Lee, H. J.; Hwang, B.; Joo, H. M. (2015). Under-ice measurements of suspended particulate matters using ADCP and LISST-Holo. *Ocean Science Journal* 50(1): 97–108. https://doi.org/10.1007/s12601-015-0008-2

Haun, S. & Lizano, L. (2015). Sensitivity analysis of sediment fluxes derived by using acoustic backscatter. *Proc. 36th IAHR World Congress*, The Hague, The Netherlands

Haun, S.; Rüther, N.; Baranya, S.; Guerrero, M. (2015). Comparison of real time suspended sediment transport measurements in river environment by LISST measurements in stationary and moving operation mode. *Flow Measurement and Instrumentation* 41: 10–17. http://dx.doi.org/dx.doi.org/10.1016/j.flowmeasinst.2014.10.009

Haun, S. & Lizano, L. (2016). Evaluation of a density current from ADCP backscatter data and LISST measurements. *Proc. River Flow 2016*, G. Constantinescu, M. García, D. Hanes (eds.), London: 875–881. ISBN 978-1-138-02913-2

Hodder, K. R. (2009). Flocculation: a key process in the sediment flux of a large, glacier-fed lake. *Earth Surface Processes and Landforms* 34(8): 1151–1163. http://dx.doi.org/10.1002/esp.1807

Hodder, K. R. & Gilbert, R. (2007). Evidence of flocculation in glacier-fed Lillooet Lake, British Columbia. *Water Research* 41(12): 2748–2762. http://dx.doi.org/10.1016/j.watres.2007.02.058

Huss, M.; Bauder, A.; Funk, M.; Hock, R. (2008a). Determination of the seasonal mass balance of four Alpine glaciers since 1865. *Journal of Geophysical Research: Earth Surface* 113(F1): 1–11. http://dx.doi.org/10.1029/2007jf000803

Huss, M.; Farinotti, D.; Bauder, A.; Funk, M. (2008b). Modelling runoff from highly glacierized alpine drainage basins in a changing climate. *Hydrological processes* 22(19): 3888–3902. http://dx.doi.org/10.1002/hyp.7055

Huss, M.; Zemp, M.; Jörg, P.C.; Salzmann, N. (2014). High uncertainty in 21st century runoff projections from glacierized basins. *Journal of Hydrology* 510: 35–48. http://dx.doi.org/10.1016/j.jhydrol.2013.12.017

Hutter, K.; Wang, Y.; Chubarenko, I. P. (2011). Physics of Lakes – Volume 3: Methods of Understanding Lakes as Components of the Geophysical Environment. ISBN 978-3-319-00473-0. *Springer*, Zurich, Switzerland

IPCC (2013). Climate Change 2013 | The Physical Science Basis. *Technical Report*, Intergovernmental Panel on Climate Change (IPCC). https://www.ipcc.ch/pdf/assessment-report/ar5/wg1/WGIAR5_SPM_brochure_en.pdf (accessed: 25/04/2017)

Jay, D. A.; Orton, P.; Kay, D. J.; Fain, A.; Baptista, A. M. (1999). Acoustic Determination of Sediment Concentrations, Settling Velocities, Horizontal Transports and Vertical Fluxes in Estuaries. *Proc. IEEE 6th Working Conference on Current Measurement*, San Diego, USA. http://dx.doi.org/10.1109/ccm.1999.755251

Jenzer Althaus, J. M. I. (2011). Sediment evacuation from reservoirs through intakes by jet induced flow. *PhD Thesis*, Ecole Polytechnique Fédérale de Lausanne (EPFL). https://infoscience.epfl.ch/record/154766/files/EPFL_TH4927.pdf (accessed: 25/04/2017)

Jouvet, G.; Huss, M.; Funk, M.; Blatter, H. (2011). Modelling the retreat of Grosser Aletschgletscher, Switzerland, in a changing climate. *Journal of Glaciology* 57(206): 1033–1045. http://dx.doi.org/10.3189/002214311798843359

Kostaschuk, R.; Best, J.; Villard, P.; Peakall, J.; Franklin, M. (2005). Measuring flow velocity and sediment transport with an acoustic Doppler current profiler. *Geomorphology* 68(1-2): 25–37. http://dx.doi.org/10.1016/j.geomorph.2004.07.012

Latosinski, F.; Szupiany, R. N.; García, C. M.; Guerrero, M.; Amsler, M. L. (2014). Estimation of concentration and load of suspended sediment in a large river by means of doppler technology. *Journal of Hydraulic Engineering* 140(7): 04014023. https://doi.org/10.1061/(asce)hy.1943-7900.0000859

Lee, J.; Liu, J. T.; Hung, C.-C.; Lin, S.; Du, X. (2016). River plume induced variability of suspended sediment particle characteristics. *Marine Geology* 380: 219–230. https://doi.org/10.1016/j.margeo.2016.04.014

Meile, T.; Bretz, N.-V.; Imboden, B.; Boillat, J.-L. (2014). Chap. 29 – Reservoir sedimentation management at Gebidem dam (Switzerland): 245–255. In: A. Schleiss; G. de Cesare; M. J. Franca; M. Pfister (eds.) Reservoir Sedimentation. ISBN 978-1-138-02675-9. *Taylor & Francis Group*, London, England.

Menczel, A. & Kostaschuk, R. (2013). Chap. 24 – Interfacial Waves as Coherent Flow Structures associated with Continuous Turbidity Currents: Lillooet Lake, Canada: 371–383. In: J. G. Venditti; J. L. Best; M. Church; R. J. Hardy (eds.) ISBN 978-1-119-96277-9. *John Wiley & Sons*, Ltd, Burnaby, Canada

Micheletti, N.; Lane, S. N. (2016). Water yield and sediment export in small, partially glaciated Alpine watersheds in a warming climate. *Water Resources Research* 52(6): 4924–4943. http://dx.doi.org/10.1002/2016wr018774

Mikkelsen, O.A.; Pejrup, M. (2000). In situ particle size spectra and density of particle aggregates in a dredging plume. *Marine Geology* 170(3): 443–459. http://dx.doi.org/10.1016/s0025-3227(00)00105-5

Moate, B. D.; Thorne, P. D. (2009). Measurements and inversion of acoustic scattering from suspensions having broad size distributions. *The Journal of the Acoustical Society of America* 126(6): 2905–2917. https://doi.org/10.1121/1.3242374

Moore, S.A. (2011). Monitoring flow and fluxes of suspended sediment in rivers using side-looking acoustic Doppler current profilers. *PhD Thesis*, Université de Grenoble. http://www.theses.fr/2011GRENU043.pdf (accessed: 25/04/2017)

Ortmanns, C. (2006). *Entsander von Wasserkraftanlagen* ('Desanders of hydropower plants'). *PhD Thesis, VAW-Mitteilung 193*, Laboratory of Hydraulics, Hydrology and Glaciology (VAW), H.-E. Minor (ed.), ETH Zürich, Switzerland. https://www.ethz.ch/content/dam/ethz/special-interest/baug/vaw/vaw-dam/documents/das-institut/mitteilungen/2000-2009/193.pdf (accessed: 25/04/2017; in German)

Riihimaki, C. A.; MacGregor, K. R.; Anderson, R. S.; Anderson, S. P.; Loso, M. G. (2005). Sediment evacuation and glacial erosion rates at a small alpine glacier. *Journal of Geophysical Research* 110(F3). http://dx.doi.org/10.1029/2004jf000189

Santos, A. I.; Oliveira, A.; Zacarias, N.; Pinto, J. P.; Ribeiro, M. (2014). Suspended sediment transport patterns in the inner shelf – S. Pedro de Moel (Portugal). *Journal of Sea Research* 93: 47–56. http://dx.doi.org/10.1016/j.seares.2014.04.009

Sassi, M. G.; Hoitink, A. J. F.; Vermeulen, B. (2012). Impact of sound attenuation by suspended sediment on ADCP backscatter calibrations. *Water Resources Research* 48(9). http://dx.doi.org/10.1029/2012wr012008.

Schleiss, A.; Feuz, B.; Aemmer, M.; Zünd, B. (1996). Verlandungsprobleme im Stausee Mauvoisin ('Reservoir sedimentation problems in Lac de Mauvoisin'). *Proc. Verlandung von Stauseen und Stauhaltungen, Sedimentprobleme in Leitungen und Kanälen ('Sedimentation in Reservoirs, Pipes and Conduits'), VAW-Mitteilung 142*, D. Vischer (ed.) ETH Zürich, Switzerland: 37–58. https://www.ethz.ch/content/dam/ethz/special-interest/baug/vaw/vaw-dam/documents/das-institut/mitteilungen/1990-1999/142.pdf (accessed: 25/04/2017; in German)

Schleiss, A.; de Cesare, G.; Jenzer Althaus, J. M. I. (2010). Verlandung der Stauseen gefährdet die nachhaltige Nutzung der Wasserkraft ('Reservoir sedimentation threatens the sustainable use of hydropower'). *Wasser Energie Luft* 102: 31–40. https://infoscience.epfl.ch/record/147714/files/Schleiss_DeCesare_Jenzer_wel_2010_Verlandung.pdf (accessed: 25/04/2017; in German)

SCNAT (2016). Brennpunkt Klima Schweiz. Grundlagen, Folgen und Perspektiven. ('Focus Climate Switzerland. Basics, Consequences and Perspectives'). Swiss Academy of Sciences, *Swiss Academies Report* 11 (5). http://www.naturalsciences.ch/uuid/289496e5-c703-5917-ad42-1abd05b8fe36?r=20161005181841_1484061355_0d8762b6-48e9-5186-a15e-a89c7ed607ff (in German, accessed: 25/04/2017)

SGHL & CHy (2011). Auswirkungen der Klimaänderung auf die Wasserkraftnutzung | Synthesebericht ('Effects of climate change on hydropower use | synthesis report'). *Beiträge zur Hydrologie der Schweiz* 38, Schweizerische Gesellschaft für Hydrologie und Limnologie (SGHL) und Hydrologische Kommission (CHy). http://www.hydrologie.unibe.ch/projekte/Synthesebericht.pdf (accessed: 25/04/2017; in German)

SonTek (2000). SonTek/YSI Acoustic Doppler Profiler. Technical documentation, SonTek

SonTek (2017). RiverSurveyor S5/M9 SmartPulseHD®* Feature. Technical Note, SonTek

Stott, T. & Mount, N. (2007). Alpine proglacial suspended sediment dynamics in warm and cool ablation seasons: Implications for global warming. *Journal of Hydrology* 332(3/4): 259–270. http://dx.doi.org/10.1016/j.jhydrol.2006.07.001

Swift, D. A.; Nienow, P. W.; Hoey, T. B. (2005). Basal sediment evacuation by subglacial meltwater: suspended sediment transport from Haut Glacier d'Arolla, Switzerland. *Earth Surface Processes and Landforms* 30(7): 867–883. http://dx.doi.org/10.1002/esp.1197

Thevenot, M. M.; Prickett, T. L.; Kraus, N. C. (1992). Tylers Beach, Virginia, Dredged Material Plume Monitoring Project 27 September to 4 October 1991. *Technical Report DRP-92-7*, U.S. Army Corps of Engineers. http://handle.dtic.mil/100.2/ADA261036 (accessed: 25/04/2017)

Unverricht, D.; Nguyen, T. C.; Heinrich, C. Szczuciński, W.; Lahajnar, N.; Stattegger, K. (2014). Suspended sediment dynamics during the inner-monsoon season in the subaqueous Mekong Delta and adjacent shelf, southern Vietnam. *Journal of Asian Earth Sciences* 79: 509–519. https://doi.org/10.1016/j.jseaes.2012.10.008

Uhlmann, B.; Jordan, F.; Beniston, M. (2013). Modelling runoff in a Swiss glacierized catchment | Part II: daily discharge and glacier evolution in the Findelen basin in a progressively warmer climate. *International Journal of Climatology* 33(5): 1301–1307. http://dx.doi.org/10.1002/joc.3516

Urick, R. J. (1975). Principles of Underwater Sound. ISBN 978-0932146625. *McGraw Hill*, New York, USA

Wisser, D.; Frolking, S.; Hagen, S.; Bierkens, M. F. P. (2013). Beyond peak reservoir storage? A global estimate of declining water storage capacity in large reservoirs. *Water Resources Research* 49(9): 5732–5739. http://dx.doi.org/10.1002/wrcr.20452

Wood, T.M.; Gartner, J.W. (2010). Use of acoustic backscatter and vertical velocity to estimate concentration and dynamics of suspended solids in Upper Klamath Lake, South-Central Oregon: Implications for Aphanizomenon flos-aquae. Scientific Investigations Report 2010-5203, U. S. Geological Survey. https://pubs.usgs.gov/sir/2010/5203/pdf/sir20105203.pdf (accessed: 25/04/2017)

Wood, M. S. & Teasdale, G. N. (2013). Use of Surrogate Technologies to Estimate Suspended Sediment in the Clearwater River, Idaho, and Snake River, Washington, 2008-10. *Scientific Investigations Report 2013-5052*, U.S. Department of the Interior, U.S. Geological Survey. http://pubs.usgs.gov/sir/2013/5052/pdf/sir20135052.pdf (accessed: 25/04/2017)

Woodward, J. C.; Porter, P. R.; Lowe, A. T.; Walling, D. E.; Evans, A. J. (2002). Composite suspended sediment particles and flocculation in glacial meltwaters: preliminary evidence from Alpine and Himalayan basins. *Hydrological Processes* 16(9): 1735–1744. http://dx.doi.org/10.1002/hyp.361

Xu, J.; Sequeiro, O. E.; Noble, M. A. (2014). Sediment concentrations, flow conditions, and downstream evolution of two turbidity currents, Monterey Canyon, USA. *Deep Sea Research I* 89: 11–34. http://dx.doi.org/10.1016/j.dsr.2014.04.001

Yuan, Y.; Wei, H.; Zhao, L.; Jiang, W. (2008). Observations of sediment resuspension and settling off the mouth of Jiaozhou Bay, Yellow Sea. *Continental Shelf Research* 28(19): 2630–2643. https://doi.org/10.1016/j.csr.2008.08.005